Instituto Tecnológico y de Estudios Superiores de Monterrey

Campus Estado de México

School of Engineering and Sciences

Synthesis and Biotriborheological Characterization of Shea Butter Solid Lipid Nanoparticles in Topical Formulation

A thesis presented by

Jose Ivan Aviles Castrillo

Submitted to the
School of Engineering and Sciences
in partial fulfillment of the requirements for the degree of

Master of Science

In

Nanotechnology

Atizapán de Zaragoza, Estado de México, November 23th, 2020

Dedication

Parents, professors, brothers and friends, thanks for all your unconditional confidence, support, patience, and encouragement. You were my main motivation for pushing through this work.

I would like to dedicate this thesis to my parents due to without them I would not be the person I am today.

Acknowledgements

I would like to acknowledge **Tecnológico de Monterrey** for being able to carry out this project, admission to my master's degree in nanotechnology, and the facilities granted.
Additionally, I am thankful to **CONACYT** to grant me the maintenance scholarship during my master's degree. Further, I would like to thank **COMECYT** for the support given to the project.
I am very grateful to **Dr. Dora Medina** for her unconditional support, the facility of carrying out this project, training, and all her dedication to this project; her time invested in my project reading, correcting, and giving ideas. Further, for having believed in me, allowing me to work with her, and granting me the opportunity to attend various conferences, as well as the publication of an article.
I thank **Dr. David Quintanar** for his support before and during the research project, for the facilities of the Laboratorio de Posgrado en Tecnología Farmacéutica, for his time invested in the project, his observations, for his patience, believe in me and suggestions.
I wish to acknowledge **Dr. Anai Valencia**, first for agreeing to be a member of the evaluation committee of this project, as well as her valuable suggestions and support in the realization of this thesis project.
I would also like to thank **Dr. Heriberto Cruz** for his help in the development of this project, his advice, and suggestions, as well as various support.
I would like to acknowledge **Dr. Ricardo Cisneros** for his support to carry out atomic force microscopies.
I would like to thank my dear friend and colleague **Katya** for her support and accompaniment before and during this project, for her advice, suggestions, and especially for helping me to be a better person.
I also want to thank **David Alfonso** for his unconditional help, for always being there, giving me support and advice, and chiefly for his patience when listening to my problems.
Furthermore, I would like to thank my brothers, **Bere, Emiliano, Neto, Josue, and Emanuel.** Thanks to your unconditional support and love, I was able to do everything I have done today.
I want to thank my parents, **Blanca and Ernesto**, for their continuous support. Actually, I am very grateful to God for having put me in their family because if it weren't for them I would not be the person I am today.
I am grateful to my colleagues; both **from Dr. Dora's research group and Dr. David's lab**, for their advice, help, fraternity, and especially companionship during this research project.
Finally, I want to thank my friends, **Arturo, Enrique, Miguel, Cristian, Manuel, Itzel, Ruth, and Diego** for always being there to support me in everything.

Synthesis and Biotriborheological Characterization of Shea Butter Solid Lipid Nanoparticles in Topical Formulation

by

Jose Ivan Aviles Castrillo

Abstract

Solid Lipid Nanoparticles (SLN) are pharmaceutical delivery system and pharmaceutical formulation that provide great biocompatibility and efficiency of encapsulation. The current challenge is the storage of these due to the time they agglomerate reducing their properties. An effective way to validate its stability in storage is conducting rheology studies. Shea Butter SLN is used, with the purpose of having a higher antioxidant effect. It has been performed the synthesis, by hot homogenization technique, with an excellent stability. We validated its penetration capacity and perform different characterizations as for example Atomic Force Microscopy (AFM), Confocal Microscopy, Scanning Electron Microscopy (SEM), DSC, DLS and Zeta potential. It gave us an mean particle size of 213 nm, with a zeta potential of -40 mV and obtaining a circular morphology; Therefore, we can affirm that a correct synthesis of these nanoparticles was carried out, due to their size and stability since after 3 months of storage they did not show significant growth. Because of Confocal Microscopy studies, due to their property that SLNs are auto-flowering, it was possible to validate that Shea Butter Solid Lipid Nanoparticles can penetrate the epidermis. Triborheological studies were carried out such as Oscillatory stress sweep, Viscosity/shear rate profile, Normal stress profile and Sliding speed sweep in this way we identify and quantify the impact of Solid Lipid Nanoparticles in topical formulations. It was discovered that SLNs had lower Coefficient of Friction than those containing bulk lipids. SLNs in topical formulations have potential applications in the cosmetic as anti-aging agents this due to its antioxidant properties, skin occlusion, increased skin hydration and potential anti-inflammatory properties.

List of Figures

List of Tables

Contents

Chapter 1

Introduction

1.1 Introduction

Solid Lipid Nanoparticles (SLNs) are pharmaceutical delivery systems that allow the nanoencapsulation of drugs, offering highly efficient protection of their constituents due to their thermochemical stability, compared to liposomes [1], emulsions [2], and polymeric nanoparticles [3]. They offer significant such skin occlusion, enhanced skin moisture and elasticity, inhibit UV rays effects, drug targeting, and improved durability of drug agents [3–6]. As in the synthesis, organic solvents are not employed and the safety of the compounds used for their synthesis, are approved by FDA [7].

The hot homogenization technique is a method for the synthesis of SLNs in which the raw lipid is heated from 5 ° C to 10 ° C above the lipid melting temperature, producing that viscosity decreases and smaller particle size can be generated. Afterward, the hydrophilic surfactant is added, and a co-surfactant can be joined to improve the stability of the SLNs, at the identical temperature of the lipid, achieving a pre-emulsion. Using a high shear device, the emulsion is formed, this can be repeated several times to obtain the desired PDI and size. This technique is the most used to synthesize SLNs, due to its easy industrial scalability and its efficiency in terms of particle sizes and PDI [8].

Currently, maintaining SLNs is a challenge. Various methods have been performed to investigate particle stability, such as zeta potential measurement, which is an analysis of the magnitude of the electrostatic, charge repulsion or affinity between particles [9]. When nanoparticles are unstable, they tend to agglomerate, causing clusters of particles, and increase their particle size; generating that these

SLNs lose their properties, and sometimes a phase separation can be detected [10,11].

The stability of colloidal nanoparticles is operated by the equilibrium of electrosteric forces of the charged particles; thus, it can be examined employing zeta potential analysis [12]. The evaluation of the variations in zeta potential values through changes in pH and ionic concentration must be studied thoughtfully, as it does not rely on a simple relation [13]. Due to rise electrostatic repulsion, agglomeration is inhibited; a suspension of particles possessing a great absolute value of zeta potential is more stable concerning those with a lower absolute zeta potential [14].

Oxidants, although chemically unstable and highly toxic to cells, are produced under standard conditions inside cells. Therefore, a healthy metabolism is a source of free radicals. Oxidants can come from outside, either directly or as a consequence of the metabolism of certain substances [15].

Oxidizing substances can act on any molecule. The interaction of oxidants with these molecules ,aka oxidative stress, causes structural modification, which leads to altered functionality [16].

Harman established in 1956 [15] that aging was caused by the oxidative action of free radicals. Therefore, antioxidants can be administered to decrease the effects of aging.

Shea butter is known to have favorable effects on health owing to their antioxidation capability, inflammatory reduction, inhibition of DNA damage, and induction of insulin production in the pancreas [17–20].

Shea butter is obtained from the seeds of Karité (Vitellaria paradoxa), mainly located in western Africa [21]. Its melting point is 37–39.5 ° C, and its main compounds are palmitic acid (3–4%), stearic acid (40–45%), oleic acid (44–47%), linoleic acid (5.5-6%) and Vitamin E (5–15 %), having great anti-inflammatory and antioxidant properties [22].

The skin is the most extensive organ of the human and possesses selective permeability. It is formed of three different functional layers (Fig. 1); epidermis, dermis, and hypodermis[23].

Epidermis, hair follicles, dermis and sweat glands make up the skin, the stratum corneum is the most external lipid layer, producing a powerful obstacle to the admission of substances into the body. An encouraging approach to increase the diffusion through the stratum corneum is to utilize nanosystems as their lipophilicity facilitates crossing the entire lipid layer [24].

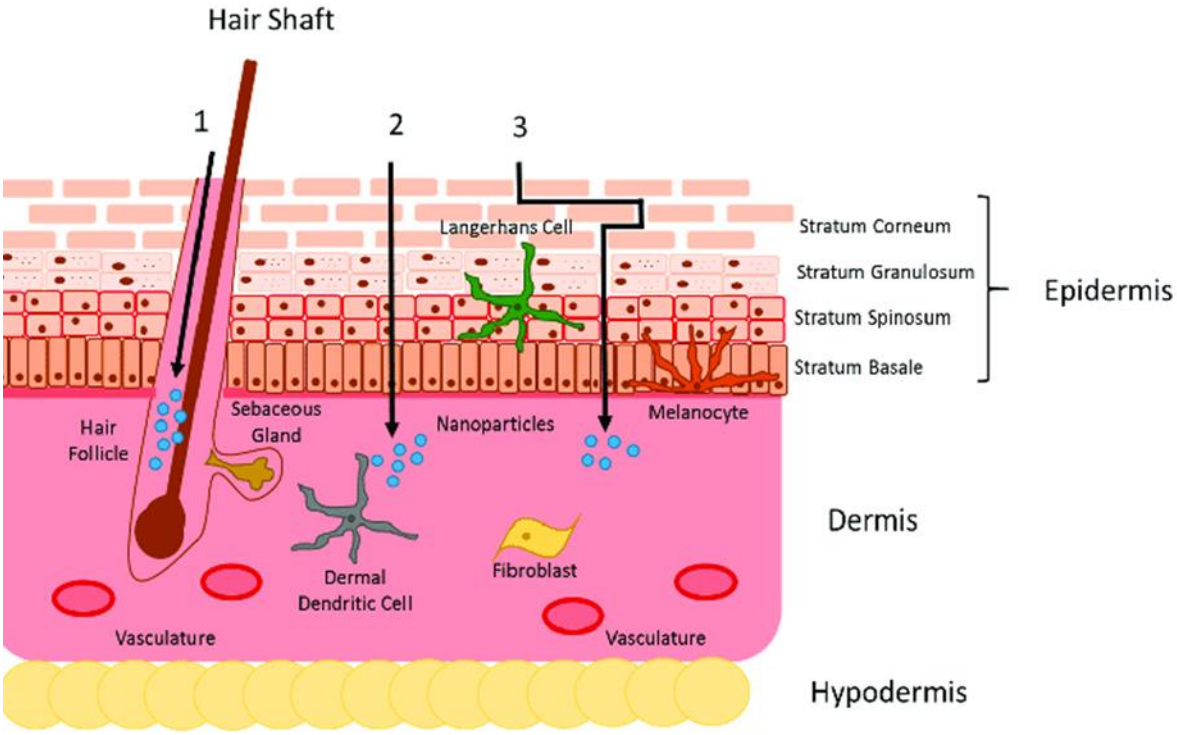

Fig. 1 Skin layers diagram

As the peripheral organ of our body, our skin is a defense defending us from dangerous vulnerability to solar ultraviolet radiation and air pollutants. This susceptibility ends in harm to the nucleus of the cell itself and in the production of reactive oxygen species that respond with relevant molecules in connective tissue and cell membranes [25].

Habitual UV-induced damage outcomes in the manner of precipitate aging of the epidermis with wrinkles, a dry, leather-like texture, and lack of elasticity. It is possible to have inflammatory skin diseases like atopic dermatitis [26].

The skin typically employs a diversity of antioxidants that associate with varied levels of oxidative processes to scavenge and eliminate free radicals and oxidatively spolied molecules [27]. Several kinds of investigations advise that oxidative stress may produce the creation of proinflammatory cytokines, which, in tum, may promote the cellular levels of ROS.

This wicked cycle ends in the continuous accrual of oxidative stress and inflammation throughout consecutive skin aging. Consequently, oxidative stress and inflammation seem to be a role in age. Nevertheless, this antioxidant protection is conquered by the oxidative stress of excessive UV exposure, aside from external factors [28].

Opportunely, employing high concentrations of natural, local antioxidants can succeed and fix this damage. Utilized topically, far higher densities are accomplished in the skin than regularly possible. Moreover, once incorporated, the antioxidants cannot be removed, exuded, or rubbed off giving strength for up to numerous days, through improving sunscreens that must be implemented periodically. Aging process cannot be shifted as yet, it is reasonable to pause its onset by fighting the increase of ROS and inflammation by reservoirs of antioxidants (Fig. 2) [29].

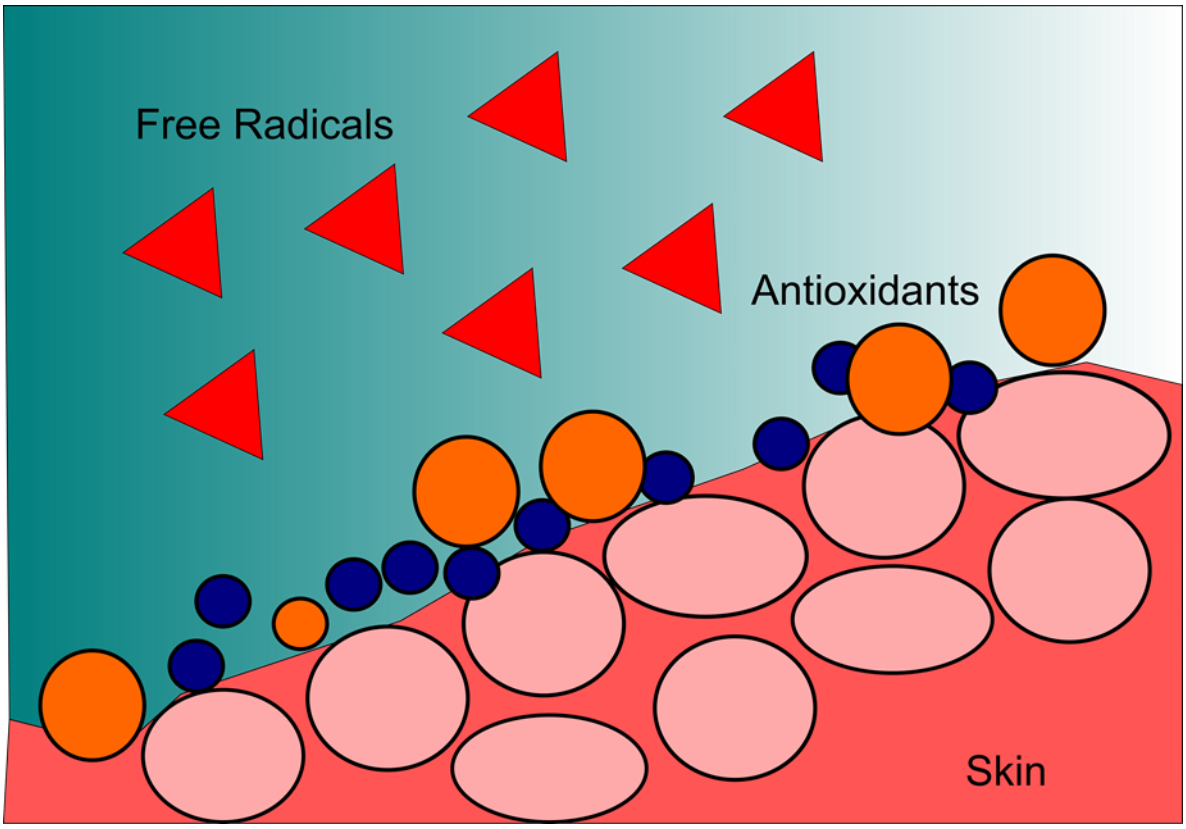

Fig. 2 Antioxidant mechanism over skin

Atopic dermatitis is a usual recidivist chronic inflammation of the skin. The term atopic means the acquired tendency of sufferers from this disease to generate immunoglobulin E antibodies in answer to environmental or food allergens such as house dust, pollen, mites, and unusual ingested proteins.

Because of the potential of this disease to originate relapsing episodes of extreme pruritis in dermatitis, it could be a major problem of psychosocial difficulties for the patients and their families. One way to treat this condition is through emollient agents [30–34].

The emollient effect is the physiological consequence of producing a light layer on the epidermis surface to limit moisture dissipation to preserve the hydration and the skin's flexible capacity. The perfect emollients for the epidermis are sebum and lipids, which shield moisture by forming a lipid coating on the epidermis surface [35].

Pharmaceutical products that include emollients conserve the moisture in the stratum corneum and are applied as essential skincare products to maintain the skin silky. Emollient topicals are the most usual examples of these products. Emollient creams are similarly named night creams, moisturizers, or moisturizing creams. Most emollient topicals utilize water in oil (w/o) type emollients that keep a moderately high quantity of oil for an extraordinary occlusion effect [36].

To stop signs that are correlated to dehydration like skin lines and unevenness, active chemicals such as retinol, several vitamins, and astaxanthin are also incorporated to improve the products' effectiveness [37,38].

Nanotechnology-based therapeutics, such as nanoparticles, nanogels, lipid nanoparticles, nanoemulsions, nanomixtures and other nanocarriers, have been investigated as possible therapies for atopic dermatitis [39–41].

Nanoparticles and nanocarriers show to have great rheological characteristics, antimicrobial results, and capacity to repair skin diseases [42–51].

Few studies proved the penetration of the SLNs through the skin, or their reaching circulatory system or passing through hair follicles [52].

Shea butter SLNs were shown to cross the stratum corneum and thus have a higher antioxidant effect and long-term stability. They can be used as anti-aging and anti-inflammatory factors in diseases such as colitis [7].

Triborheology is a new science that combines rheology and tribology characterization. Rheology is the research of strain and flux of matter. Rheological evaluation of materials provides an overall conception about the viscoelastic flow performance of the system. It is recognized that rheology is very relevant to each material because the rheological behavior is intimately associated with the ultimate compositions of the system [53,54].

Tribology implies the examination of the aspects associated with the surface of a solid or the interface among two covers. Friction, roughness, wear, etc. denote the tribological aspects. Friction signifies the force opposing the relevant movement among pair surfaces slipping toward respective others, while wear is the destruction

of matter or strain of material while a pair of surfaces in touch have the corresponding movement among them. Between both lowering events, friction delivers the performance of mechanical arrangements that include sliding surface association. It is additionally subject to wear, which is frequently the restrictive mechanism of machine assistance life. Therefore, reduction of friction and wear results essential where high performance and more extended equipment life imply a requirement [55,56].

The knowledge of the tribological features of systems possesses a huge financial and technological interest. The losing owing to energy spread and material erosion adds up to billions of dollars yearly in all nations. Precise knowledge of tribological processes is able to present a base on which to promote standards of design and improve manufacturing efficiency. This owns previously had a notable influence on energy maintenance problems that involve the future of humankind [57].

Even if tribology has conventionally implied correlated among the surface interplay of production systems, ideas of tribology should further implied essential in the investigation of living systems. Biotriborheology denotes an example of the most innovative areas to appear in the study of tribology [58]. Biotriborhelogy works with every features of tribology involved with biological/natural systems. It is accepted as an example of the most significant factors in several biological systems, giving to the perception of how our natural systems operate. Besides, it helps in explaining how conditions advance and how therapeutic interventions should be implemented [59].

Biotriborheology is an example of the most impressive domains of tribology analysis and is an example of how it influences numerous characters of our usual experiences, from skin injuries to synthetic joints and contact lenses. In numerous situations, intercommunication with our atmosphere is dictated by tribology and in special our answer to understood friction. The performance of touch to estimate surface roughness moisture and grip is an outstanding example [60].

Furthermore, several papers have shown the efficiency of using nanoparticles as lubricant additives, the smaller the particle size, the lower the coefficient of friction. [61–66]. There are several lubrication mechanisms for nanoparticles: Rolling

mechanism, sliding mechanism, , polishing/exfoliation mechanism, mending mechanism, and protective film (Fig. 3) [67,68].

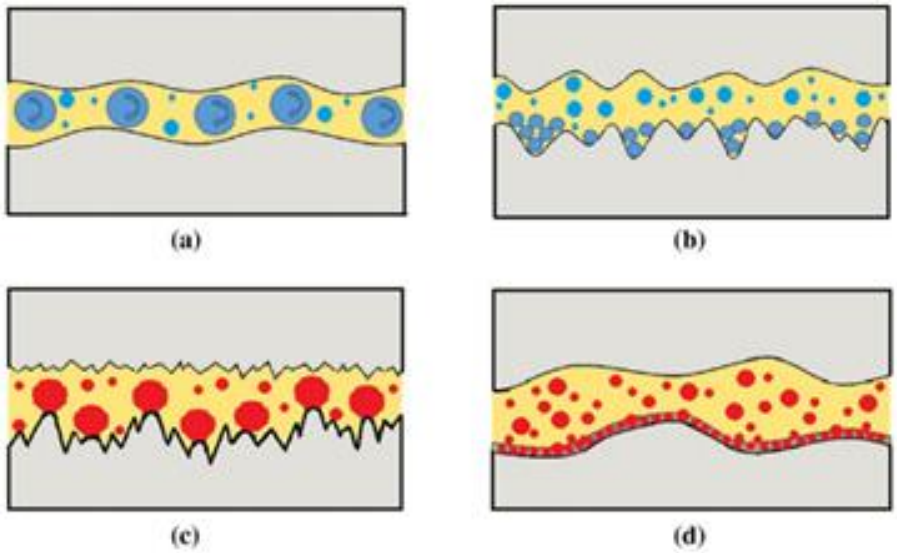

Fig. 3 Different mechanisms for improving tribological performance using nanoparticles (a) rolling mechanism; (b) mending mechanism; (c) polishing mechanism; (d) protective film [67]

One of the objectives of the topical formulations is to reduce skin scratch since it increases skin damage, this is achieved by increasing its lubricating properties, and thus reducing allergic reactions and skin irritation [69]. Thanks to the triborheological properties, the perception of topical creams can be evaluated, the nanoparticles tend to improve the lubrication properties obtaining systems with a lower COF (Coefficient of Friction), therefore the topical will have a silkier feel [70].

Additionally, with biotriborheology, the occlusion and moisture of topical formulations can be validated, and how nanoparticles influence to have triborheological behaviors which indicate that the skin has greater moisture, such as the formation of thinner and more protective layers, providing a better occlusion [69]. It should be remarked that biotriborheology studies of SLNs have never been performed, to evaluate their effect in creams or as lubricants.

In this work, the synthesis of Shea Butter SLNs with different particle size, was carried out through a hot homogenization technique, as well as our main objective which was to investigate the triborheological properties of Shea Butter SLNs in topical formulations. To have a better understanding of the physical properties of Shea butter SLNs, it is necessary to perform an in-depth characterization of their structure, flow, and lubrication [71].

Chapter 2

Materials and methodology

2.1 Materials

Shea butter was acquired from Lottush. Tween–80, triethanolamine, and Span 80 were purchased by Sigma-Aldrich. Lanolin, stearic acid, mineral oil, cetyl alcohol, propylparaben, methylparaben and glycerin were obtained from Drogueria Cosmopolita.

2.2 Synthesis of Shea Butter SLNs

The preparation is carried out by the hot homogenization method, using an in-line homogenizer to improve polydispersity and particle size [72]. The organic phase comprising 4.2% shea butter (w/v), was heated to 10 °C higher than its melting temperature; then, 1.5% Span 80 (w/v) was added while preparing the aqueous phase at the same temperature involving the lipid, Milli–Q water, and 1.5% Tween-80 (w/v) [73].

Subsequently, the organic phase was mixed to the aqueous phase by dripping to produce a pre-emulsion, which was stirred for 5 minutes and deposited into the in-line homogenizer (Fig. 4) from 5 to 20 minutes at 16,000 rpm. Finally, it was cooled to room temperature.

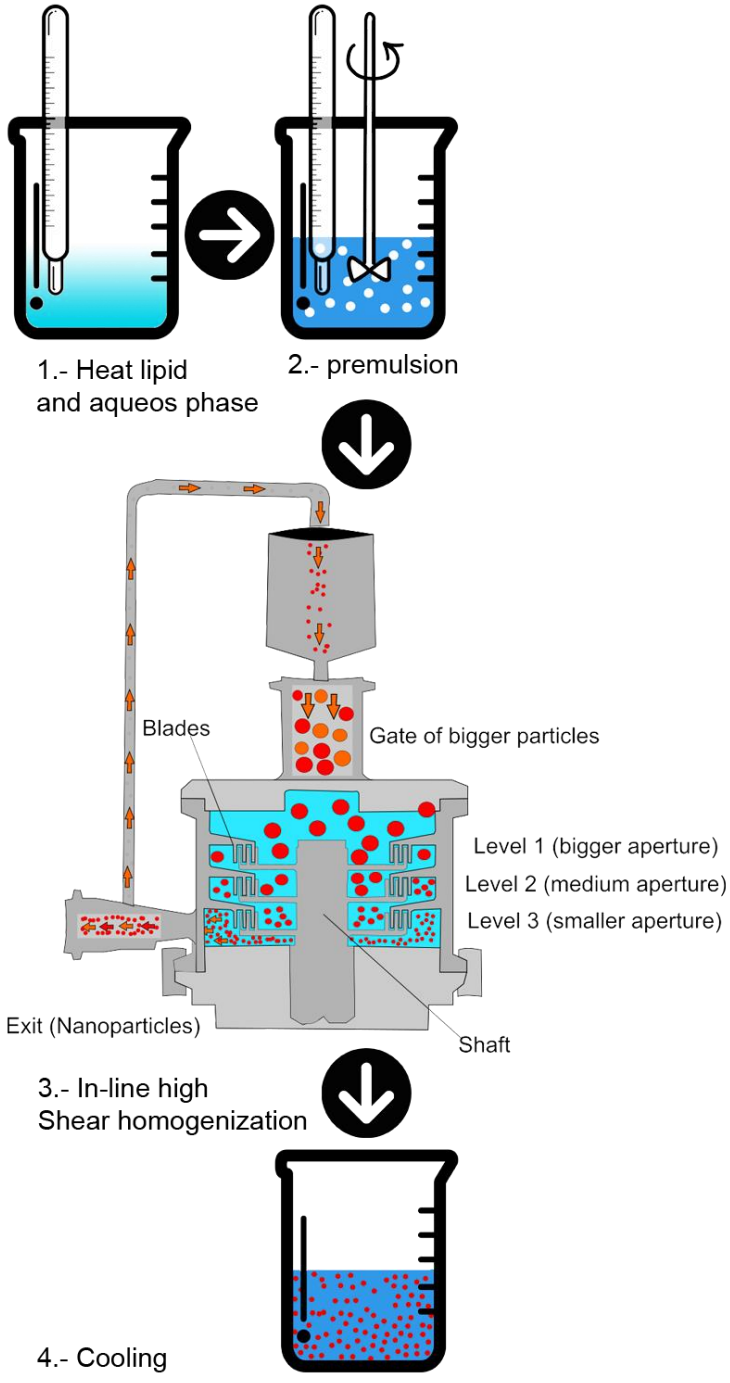

Fig. 4 Diagram of the synthesis of solid lipid nanoparticles

2.3 Characterization of Shea Butter SLNs

2.3.1 Nanoparticle size analysis

The mean diameter and polydispersity index were measured at 25°C, with 10 min of equilibrium and 90° detection angle by dynamic light scattering (DLS) using a Beckman Coulter N4 PLUS particle size analyzer. Samples were diluted to 1:1000 of the previous analysis to control the saturation. Measurements were performed in triplicate and analyzed it.

2.3.2 Electrophoretic light scattering (ELS)

The zeta potential measurements were conducted with 2 min equilibrium using a Malvern Zetasizer, nano ZS (Fig. 5); the samples were diluted to 1:100 with Milli-Q water at 25°C. All samples were analyzed in triplicate.

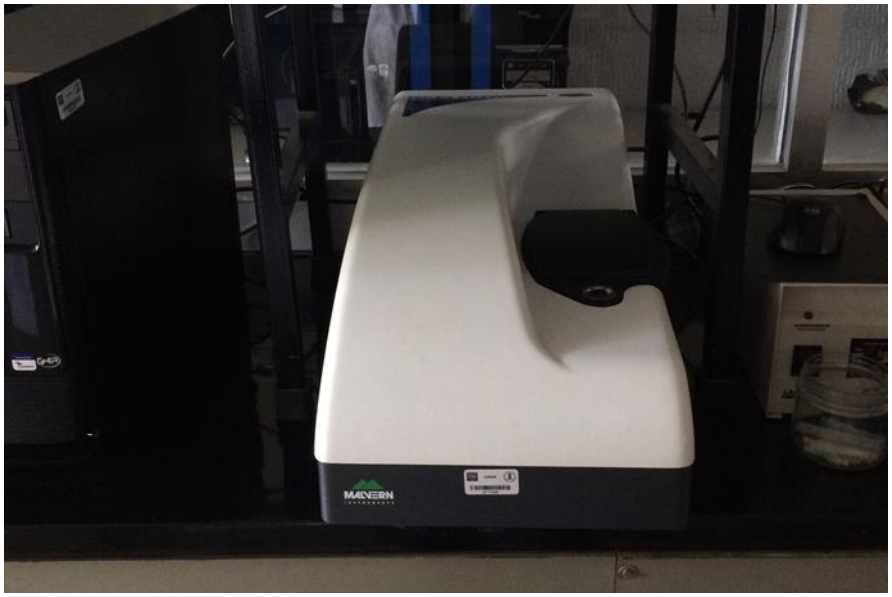

Fig. 5 Malvern Zetasizer, nano ZS

2.3.3 Atomic Force Microscopy (AFM)

The AFM images were obtained in a Multimode-8 Bruker (Fig. 6) using a cantilever RTESP-300 to scan the samples in tapping mode. Shea butter SLNs were diluted to 1:100 and 1:1000, respectively. Samples were added to the sample

holders and dried at 3 °C for 12 hours. The analysis was carried out at room temperature (25°C). The roughness was calculated using Nanoscope Analysis 1.5 from Bruker, given by:

$$\boldsymbol{R_a = \frac{1}{N}\sum_{i=1}^{N}|z_i - \bar{z}|} \quad (1)$$

$$\boldsymbol{RMS = \sigma = \sqrt{\frac{1}{N}\sum_{i=1}^{N}(z_i - \bar{z})^2}} \quad (2)$$

There are some examples where the surface roughness must depend on surface roughness where the rougher surfaces gave higher friction coefficients. But other factors of the material must be taken, such as whether the surface is soft or hard or hydrophilic or hydrophobic, to have a better study of the material [74,75].

Fig. 6 Multimode-8 Bruker

2.3.4 Scanning Electron Microscopy (SEM)

The SEM analysis of two samples of shea butter SLNs, with the smallest nanoparticle size (213 nm) was performed at several times (0-3 months). The samples 1: 1 and 1: 100 JEOL JSM 6360 (Fig. 8) was used at 20 kV. The samples were dried at 3 °C in the sample holder, to prevent agglomeration. The formulations were coated with gold on a JEOL JFC-1100E (Fig. 7).

Fig. 7 JEOL JFC-1100E

Fig. 8 JEOL JSM 6360

2.3.5 Differential Scanning Calorimetry (DSC)

The calorimetry study was carried out employing a Q20 DSC calorimeter (TA Instruments) (Fig. 9). SLNs were freeze-dried before the DSC measurement, 5 mg SLNs powder were weighed for every sample, sealed in aluminum pans with a mechanical press and scanned at a fixed rate of 5 °C/min under nitrogen from 0 to 250 °C. Temperature and energy were calibrated employing indium as a reference. For more transcendent reproducibility, it was carried out by triplicate.

Fig. 9 Q20 DSC calorimeter, TA Instruments

2.4 Triborheological Testing of Shea Butter SLNs

The rheology was performed using a TA Instruments Hybrid Rheometer DHR-3 with Cone on plate fixture and a Peltier system acting under the lower plate at a temperature of 25 °C. 3 ml of shea butter SLNs (213nm). The suspension viscosity was measured as a function of shear rate from 0.01 to 1000 1/s. The experiment was performed by triplicate for reproducibility.

The cone-on-plate viscometer comprises a cone-shaped covering and a smooth plate. Both of these surfaces can remain switched. The space that separates the cone and the plate is loaded with the lubricant and the cone angle guarantees a uniform shear rate in the gap space. The benefit of this viscometer remains that a very tiny specimen amount of solution is needed for the analysis. It could be controlled, the temperature of the fluid sample through experiments. This is

accomplished by flowing preheated or reduce the temperature of the external liquid by the Peltier plate of the viscometer. The schematic diagram of this viscometer is presented in Fig. 10 The dynamic viscosity can be calculated from the equation:

$$\boldsymbol{\eta} = \frac{\boldsymbol{kM}}{\boldsymbol{\omega}} \tag{3}$$

Where $\boldsymbol{\eta}$ is the dynamic viscosity, M is the shear torque on the cone, k is the viscometer constant, regularly provided by the company and $\boldsymbol{\omega}$ is the angular velocity

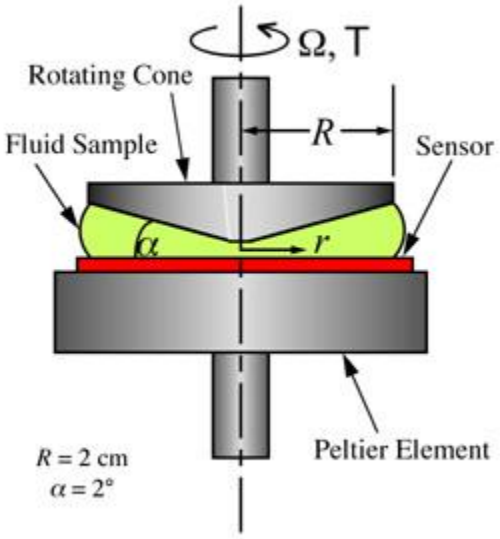

Fig. 10 Schematic diagram of a cone on plate viscometer [76].

Furthermore, triborheology of shea butter SLNs with a half-ring plate fixture was performed from 0.001 to 100 rad/s with 1 N and 3 N in the TA Instruments Hybrid Rheometer DHR-3 using a temperature of 25 °C and 3 ml of shea butter SLNs.

The frictional performance of slipping surfaces obeys a well-established model represented by the Stribeck curve. This associates the Coefficient of Friction to a series of circumstances, compared to the surfaces and the lubricant that divides them. It occurs when the determined Coefficient of Friction among both solid surfaces continues to decrease that the liquid is expressed as a lubricant. This decrease in friction or lubrication occurs in diverse methods. These can be easily

explained as boundary, fluid-film, and mixed lubrication. In watery systems, the word fluid-film lubrication is named hydrodynamic lubrication [77–79].

The distinctness among the several varieties of is lubrication and their impact on the frictional opposition to sliding remains described by a Stribeck curve. As aforementioned, the difference in the Coefficient of Friction plots as a function of the Sommerfeld number. The Stribeck curve (Fig. 11.) explains the difference in the Coefficient of Friction in words of sliding speed (v), the normal force (N), and solution viscosity ($\boldsymbol{\eta}$). These three determinants regularly develop as an individual number named the Sommerfeld number, where L is associated with a touch dimension of the sample. [80,81].

$$\boldsymbol{S} = \frac{\boldsymbol{\eta v}}{\boldsymbol{NL}} \tag{4}$$

Boundary lubrication is determined by the sliding rugosities are separated by a slim molecular layer of lubricant so that the chemical and physical characteristics of the surfaces and the lubricant are of primary concern. In boundary lubrication, the lubricant is usually competent of being adsorbed on the surfaces. In opposition, at a high Sommerfeld number, the contrary both solid surfaces are fully insulated by lubricant in the fact of fluid-film or hydrodynamic lubrication. As a consequence, friction shifts very moderately.

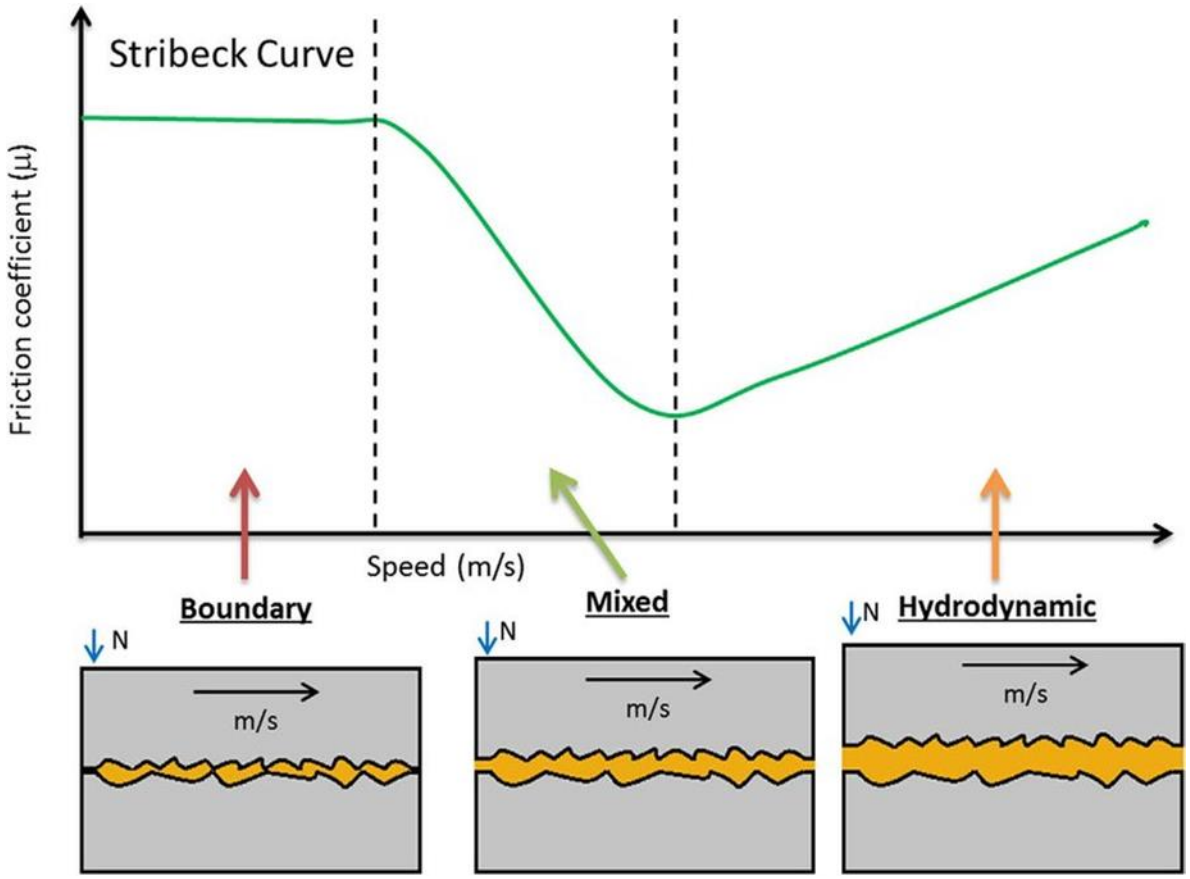

Fig. 11 Stribeck Curve

Several techniques have been recommended for examining the friction ($\boldsymbol{\mu}$) and wear. The postulate for arranging the Coefficient of Friction is the corresponding between the diverse approaches in that it is the determination of the rate of frictional force to the normal load implemented on the specimen in the frictional movement. Nevertheless, it is usually challenging to define the value of $\boldsymbol{\mu}$ for biological materials owing to their complex configuration. The underlying postulates implicated in the resolution of the Coefficient of Friction are shown in Fig. 12 [81,82].

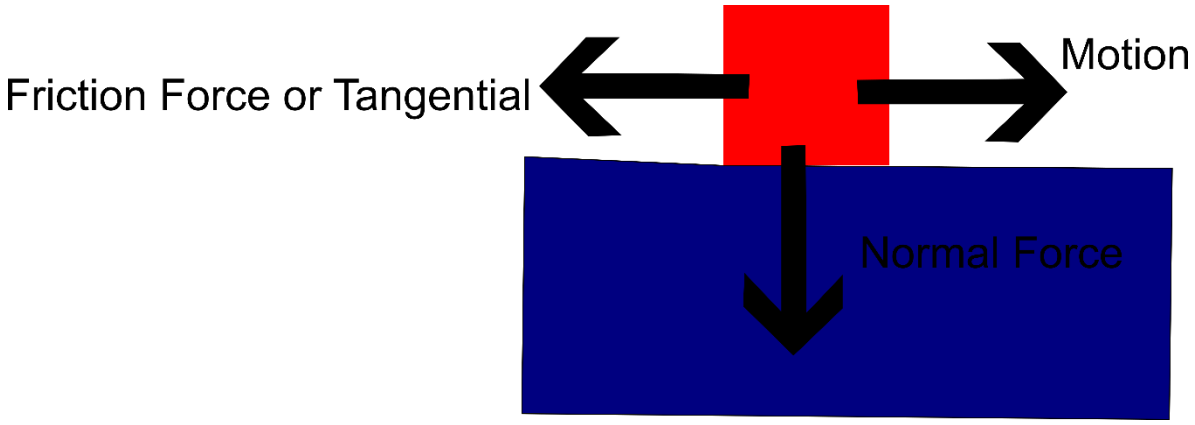

Fig. 12 Schematic of involved forces

The static friction coefficient ($\boldsymbol{\mu}$) among two hard surfaces is defined as the rate of the tangential force (F) needed to generate sliding separated by the normal force among the surfaces (N):

$$\boldsymbol{\mu} = \frac{\boldsymbol{F}}{\boldsymbol{N}} \tag{5}$$

If we want to calculate the coefficient of friction with the ring on plate geometry we use the follow formula to construct the Stribeck curves [83,84].

$$\boldsymbol{\mu} = \frac{\boldsymbol{\tau}}{\boldsymbol{\sigma}} \tag{6}$$

Where $\boldsymbol{\tau}$ is the shear stress and $\boldsymbol{\sigma}$ is the normal stress.

2.5 Preparation of Evanescent Cream (Base Cream)

It was prepared by adding 0.85% lanolin (w/w), 3.40% stearic acid (w/w), 14.87% mineral oil (w/w), 1.02% cetyl alcohol (w/w), and 0.05% propylparaben (w/w), and heating at 75 ° C with constant stirring.

Subsequently, the aqueous phase was prepared with 0.20% methylparaben (w/w), 0.85% glycerin (w/w), and 76.67% water (w/w), also heating at 75 °C with constant stirring.

Both phases were mixed at a stirring rate of 350 rpm for 10 min, 1.52% triethanolamine (w/w) was added and stirred until cooled.

2.6 Triborheological Testing of Shea Butter SLNs in Evanescent Cream

Different percentages of shea butter SLNs were added to the evanescent cream; in addition, the same concentrations were added of bulk shea butter to assess the difference among them.

Rheology was performed using a TA Instruments Hybrid Rheometer DHR-3 with Cone on plate fixture and a Peltier system acting under the lower plate at 25 °C. For 3 milliliters of Shea Butter SLN in evanescent cream, rheology experiments were performed as reported for shea butter SLNs.

Triborheological characterization was performed on TA Instruments Hybrid Rheometer DHR-3 with a half-ring plate fixture from 0.001 to 100 rad/s with 1N and 3N at 25 °C with 2 ml of Evanescent cream with and without SLNs.

2.7 Biotribo-rheological Test of Shea Butter SLN in Evanescent Cream

At First, skin from the outside of the pig's ear without thermal treatment was used, it was cleaned and separated from the cartilage with a scalpel, the excess fat was removed, and the hair was cut. Subsequently, it was cut with dissecting scissors of a size of 4cm x 4 cm. Samples were stocked in a freezer at –20 ° C.

After the samples were defrosted, they were placed in the DHR-3 rheometer using a half–ring fixture (Fig. 13). Two comparative studies were performed, one accompanied by 2 ml cream among different percentages of shea butter SLNs and the other one with 2 ml cream alongside different percentages of bulk shea butter. Experiments were carried out at velocities from 0.001 to 100 rad/s with normal forces of 0.2 N, 1 N and 3 N was used, at 25 °C.

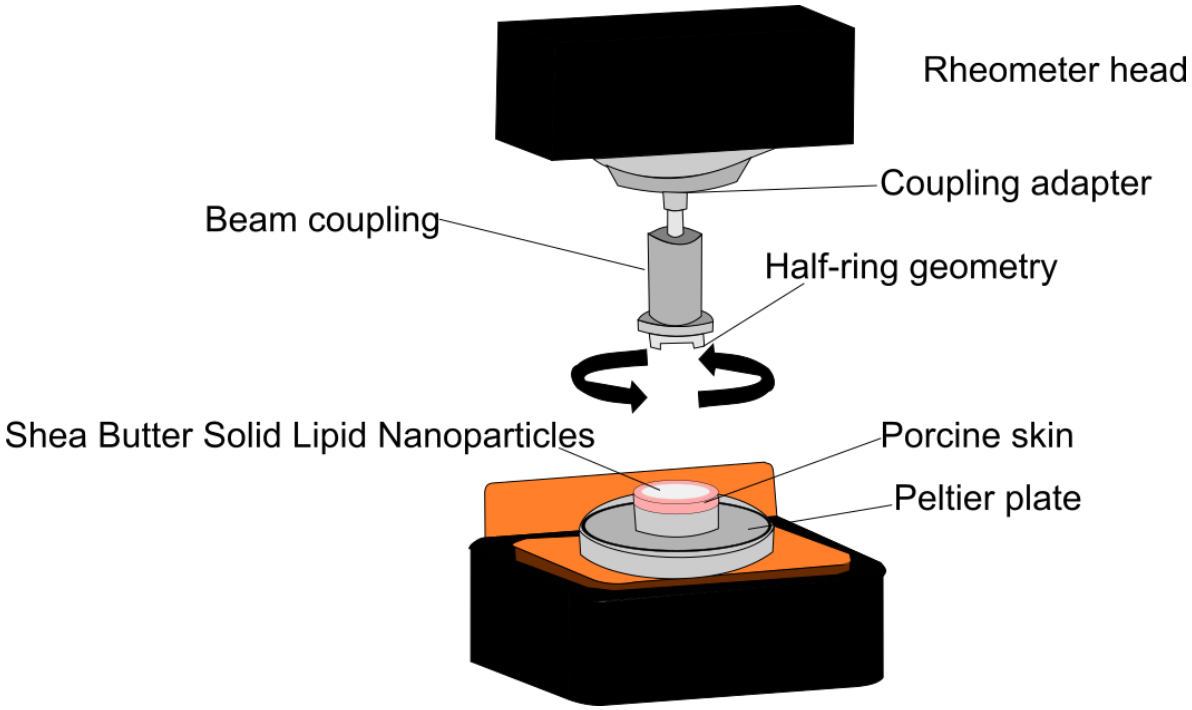

Fig. 13 Biotriborheological system

2.8 Confocal Microscopy

Confocal microscopy was performed on Zeiss LSM800, by a run of flow sweep with 2 ml of shea butter SLNs for 5 to 20 min at 25 °C; then, the skin was washed with PBS solution fine-cut with a dermatome and then taken to the microscope (Fig. 14).

At the same time, in another cut of porcine skin, shea butter SLNs were added without rubbing for 5 to 20 min, no axial force was applied, by Franz diffusion cells. It was washed in the same way with PBS solution and fine–cut with a dermatome for confocal microscopy observation.

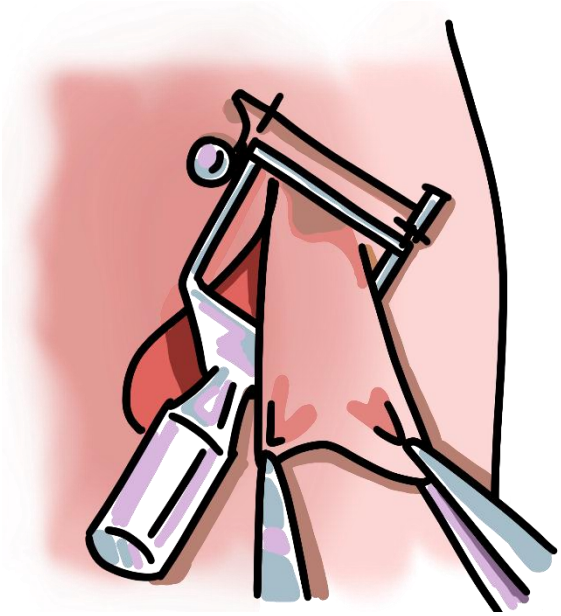

Fig. 14 Porcine skin cut with dermatome

A 480 nm filter was used, due to shea butter SLNs are autofluorescent at this wavelength and 3D z-stack function is used with layers, to validate the penetration of SLNs.

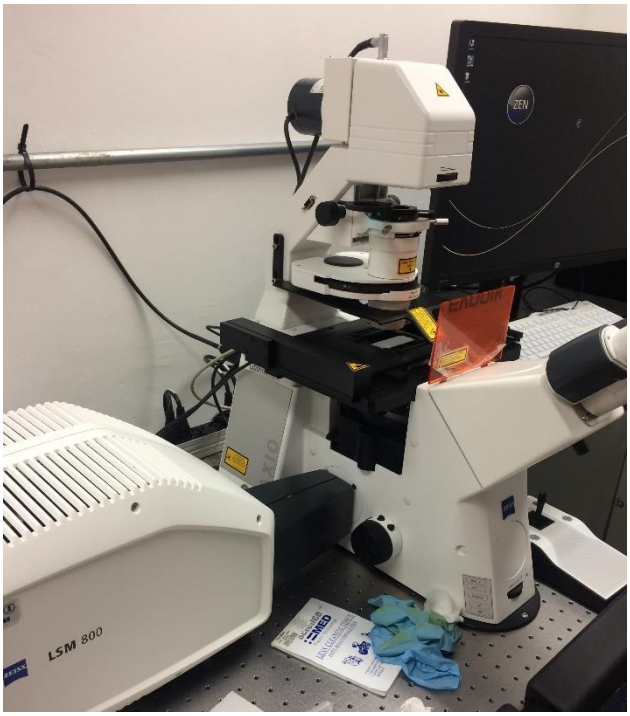

Fig. 15 Zeiss LSM800, Confocal Microscope

2.9 Statistical analysis

For statistical analysis, Minitab 19 software (2020 Minitab, LLC., Pennsylvania, USA) was used by using one-way analysis of variance, the data was evaluated at least in triplicate, and a P-value of 0.05 was regarded as significant.

Chapter 3

Results and Discussion

3.1 Nanoparticle size

To validate the particle size and its storage stability of SLNs, DLS and zeta potential studies were performed. Different particle sizes were obtained according to the time in which the homogenization was performed, the smallest size was 213 nm with the highest homogenization time (25 min). As expected, the sizes are shown in Table 1 with their PDI, homogenization time, and zeta potential.

Table 1. Physicochemical characteristics of Shea Butter Solid Lipid Nanoparticles

Batches	*Time (min)*	*Size (nm)*	*PDI*	*Zeta Potential (mV)*
1	5	320 ± 10.1	0.513 ± 0.27	-24.7 ± 0.18
2	10	276 ± 8.6	0.424 ± 0.22	-25.6 ± 0.26
3	15	232 ± 3.5	0.374 ± 0.12	-28.6 ± 0.34
4	20	221 ± 2.2	0.406 ± 0.23	-35.7 ± 0.22
5	25	213 ± 2.1	0.357 ± 0.1	-41.2 ± 0.58

The stability of SLNs was visualized for 3 months; in Fig. 16; the first 2 months showed an increase in the mean size (40 nm); the third month, a further rise in the mean size (80 nm). This is mainly due to the nature of nanoparticles which constantly tend to agglomerate over time, but these results showed that they have good stability for 3 months, confirming the synthesis of stable SLNs. For this reason, we have a steric mechanism of stability of the nanoparticles due to the addition of surfactants allowing a spatial repulsion and a reduction in the surface hydrophobicity [85–88]. This can be proved in Fig. 17, where SEM images are presented at different times

(1-3 months), indicating how the SLNs start to agglomerate, rising their particle size [89].

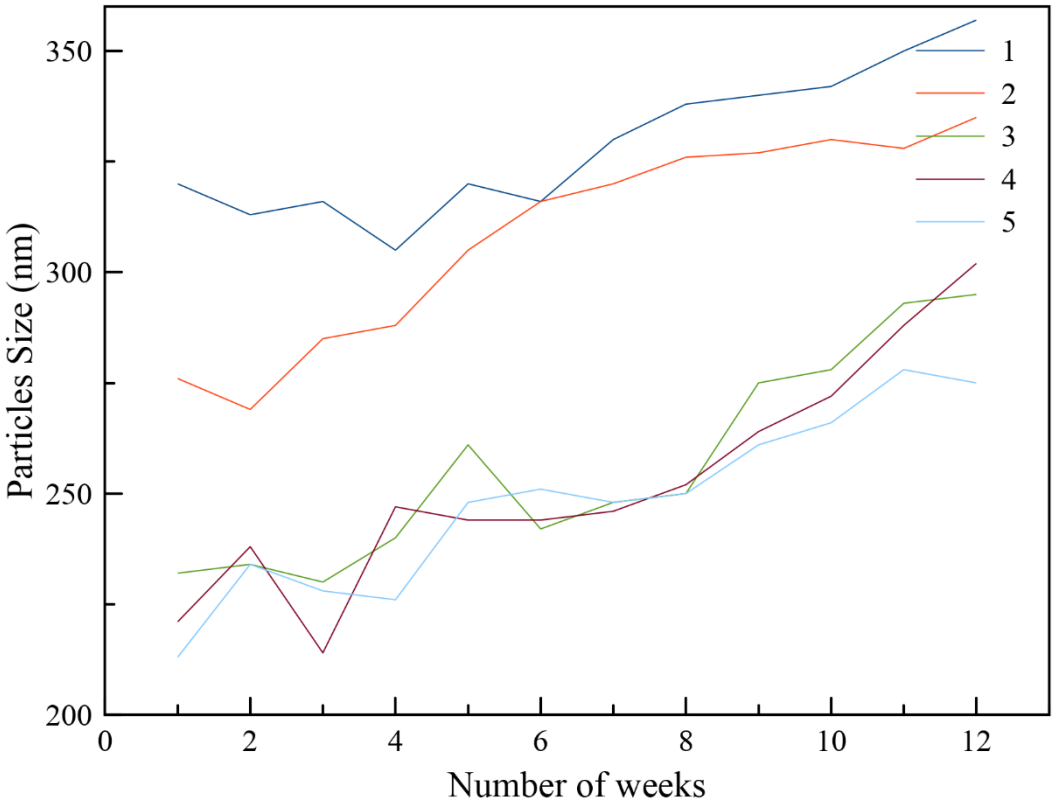

Fig. 16 Stability of Shea Butter SLNs, Mean Size in nanometers per week of each corresponding batch ±s.d. (n = 3)

This agglomeration is confirmed in previous studies [90–92], which mention that even with the use of surfactants after a prolonged time, nanoparticles tend to change their size. This is owing to Van der Waals forces, producing collision of disperser deserted particles, producing larger nanoparticles.

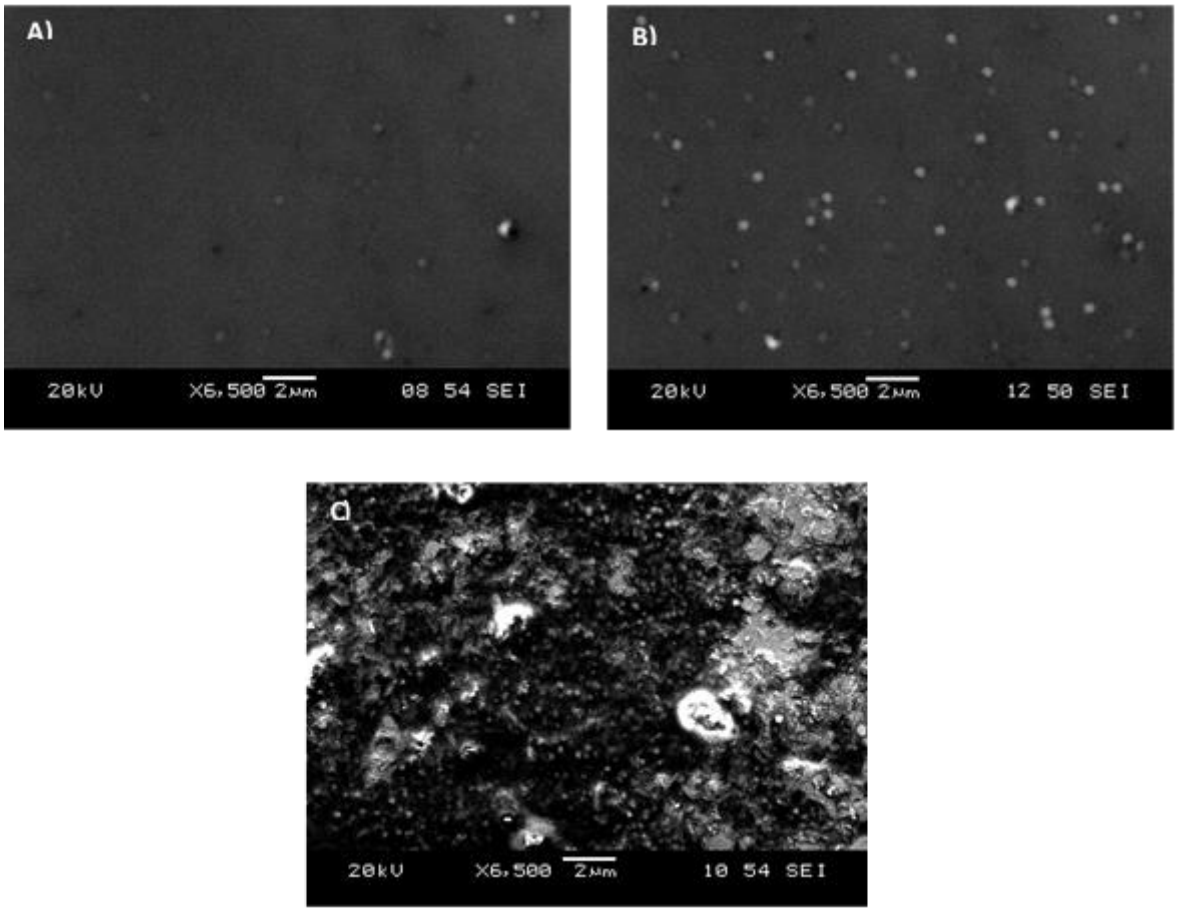

Fig. 17 SEM images of Shea Butter Solid Lipid Nanoparticles at different times, A) 1 month, B) 2 months and C) 3 months of synthesis to validate it stability

3.2 Atomic Force Microscopy

To confirm the particle size and obtain surface roughness parameters of nanoparticles, AFM characterization was executed. We selected the sample with smaller particle size (213 nm) and analyzed it in the AFM. They have a round morphology with an approximate mean size of 145 nm (Fig. 18), which agrees well with DLS measurements since DLS measures the hydrodynamic radius and small variation in the nanoparticle size is expected [93]. Although an agglomeration of SLNs can be observed, due to the characteristics of the nanoparticles that tend to agglomerate [90].

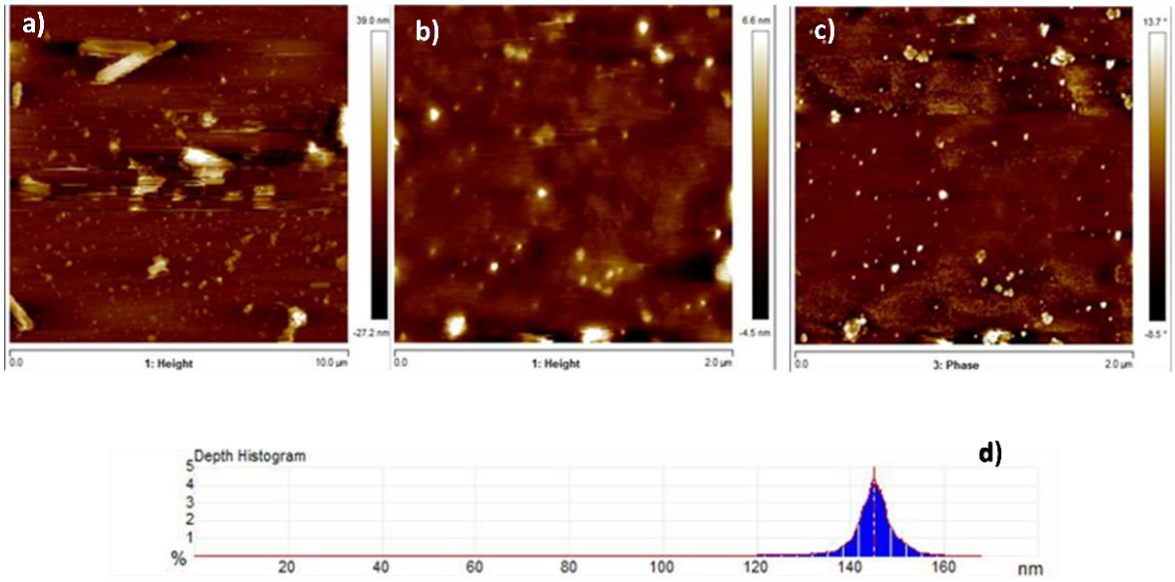

Fig. 18 AFM Images of Shea Butter SLNs with different magnifications, (a,b) top view of Shea Butter SLNs (1:1 and 1:100) ,(c) phase image, (d) Height histogram distribution based on AFM

Moreover, we have that the obtained roughness parameters are RMS = 1.13 nm, R_a = 0.662 nm and R_{max} = 17.3 nm, for an area of 2 × 2 μm^2 (Fig. 19). By comparing them with previous studies [94], it is conclude that the Shea Butter SLNs have smaller parameters, indicating that they own a lower roughness since a lower general roughness of the sample results in the lower RMS observed [95]. This helps nanoparticles to have a lower coefficient of friction as they have a lower general roughness.

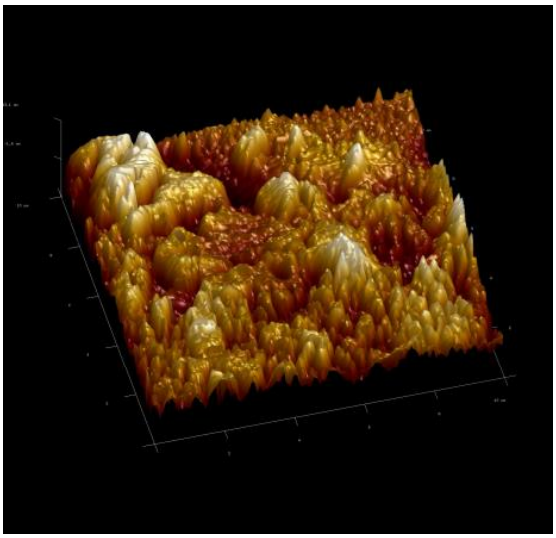

Fig. 19 3D AFM image surface roughness analysis

3.3 Scanning Electron Microscopy

It was performed Scanning Electron Microscopy to validate the morphology, formation of SLNs layers on the surface, and previous AFM and DLS characterizations. The images confirm the circular morphology of Shea Butter SLNs, furthermore, the mean particle size of SLNs can be verified (approximately 215 nm). The difference between one concentration and the other one is that with a greater concentration of SLNs, the number of agglomerates and characteristic layers of the SLNs increase[96]. Agglomeration is visualized caused by Van der Waals forces owing to the proximity of nanoparticles to each other during the drying process (Fig. 20) [97].

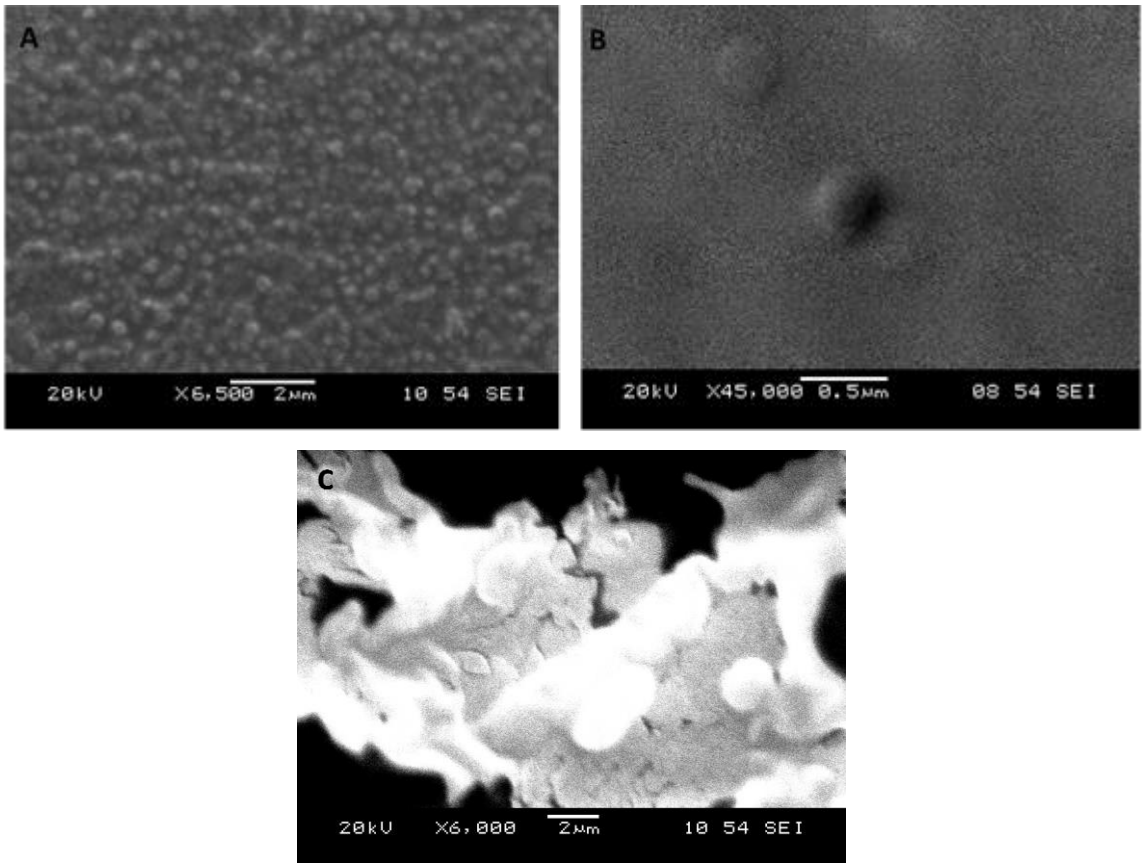

Fig. 20 SEM Images of Shea Butter Solid Lipid Nanoparticles (A,C) 1:1 and (B) 1:100, with different magnifications

In Fig. 20C, it is validated that the lipid nanoparticles tend to form layers, as reported in the literature [98], these layers help the formation of films on the surface producing a reduction in friction as it will be confirmed later in the article, with triborheological studies.

3.4 DSC characterization

To establish the correct formation of the nanoparticles and the decrease in crystallinity, DSC characterization was carried out. The thermal behavior of shea butter SLNs compared to bulk shea butter was investigated. Fig. 21 shows DSC thermograms, where bulk shea butter presents an endothermic peak at approximately 37.5 °C appropriate to its melting point, however, SLNs melting point had a shift at a inferior temperature with a maximum point at 33.5 °C. This behavior

has already been reported previously in the literature [73,99,100]. This can be described by the colloidal behavior of the lipid compared to the lipid in bulk [101]. Existing studies showed that this is because of SLNs forming a different crystal structure [16]. At these points we can observe a change in the enthalpy energies from −53.10 J/g to −38.88 J/g, indicating the formation of nanoparticles [102].

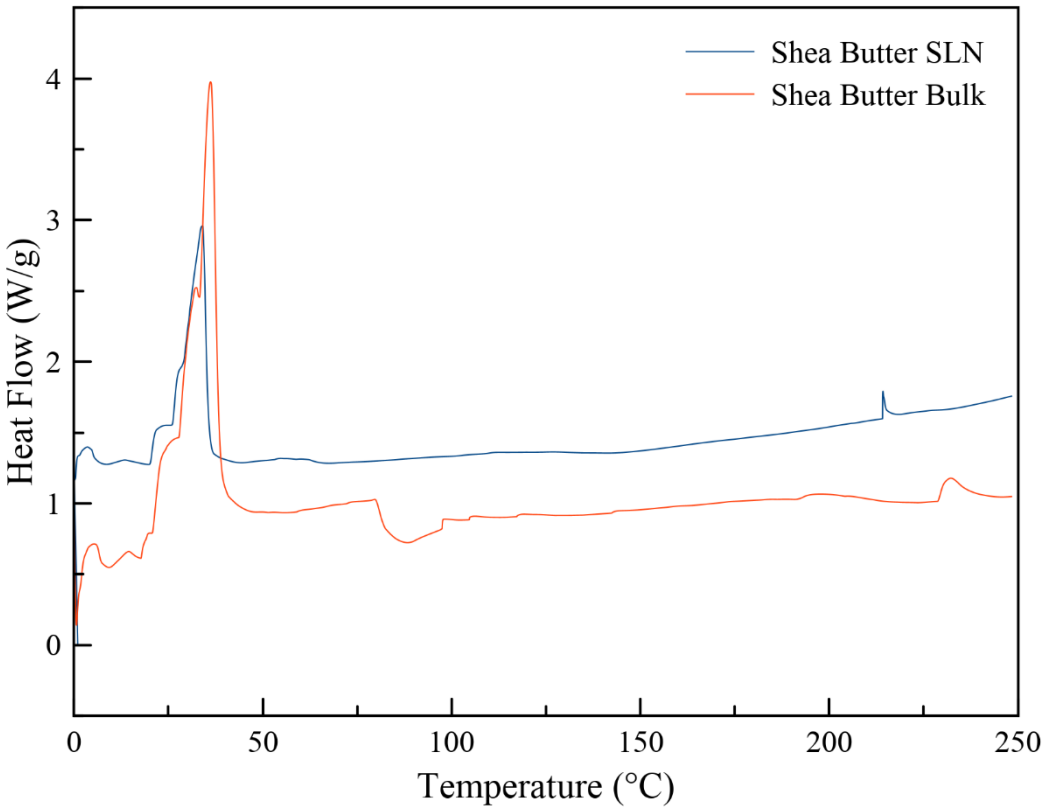

Fig. 21 Thermal analysis of Shea Butter SLNs and Bulk Shea Butter from DSC

3.5 Triborheological Tests of Shea Butter SLNs

To verify the shear-thinning rheological behavior of SLNs and the effect of particle size on their lubrication properties, triborheology studies were accomplished.

3.5.1 Rheological Testing of Shea Butter SLN

Fig. 22 shows that an increase in shear rate decreases its viscosity, as observed in previous studies [99,102]. This indicates that nanoparticles are stable due to their rheological behavior, shear thinning with a slight slope [99].

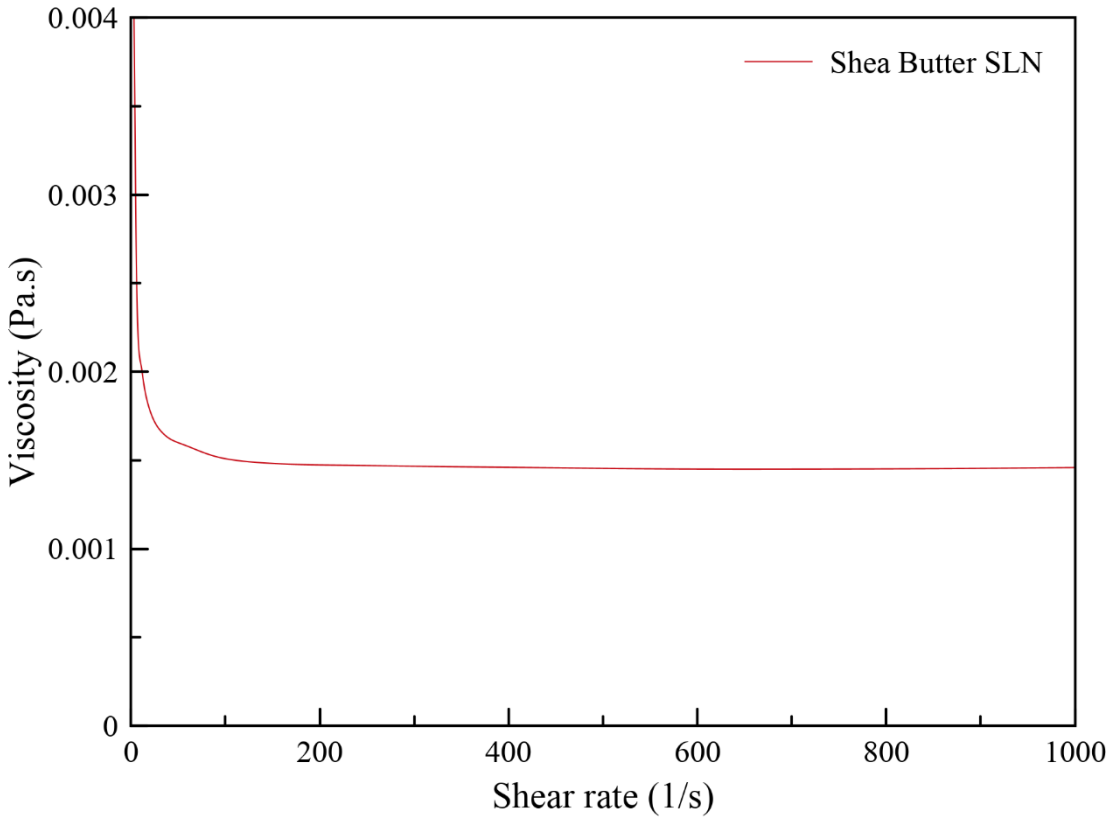

Fig. 22 Comparison of Viscosity with Shear rate of Shea Butter SLNs (213 nm)

The elastic and viscous properties of nanoparticles are important for skincare applications. The visualized curve is of a non-Newtonian fluid due to shear-thinning [103]; thus, it results in a homogenous application of SLNs and this explains its good occlusion, however, when the topical is applied on the skin, less viscosity is needed to improve its penetration, hydration and occlusion [69].

3.5.2 Triborheological Testing of Shea Butter SLNs

Fig 23a. shows that the lowest friction coefficient is the one with the smallest particle size (213 nm), mainly because smaller particle sizes favor the formation of

more uniform layers on the surface, producing a lower coefficient of friction by reducing asperities.

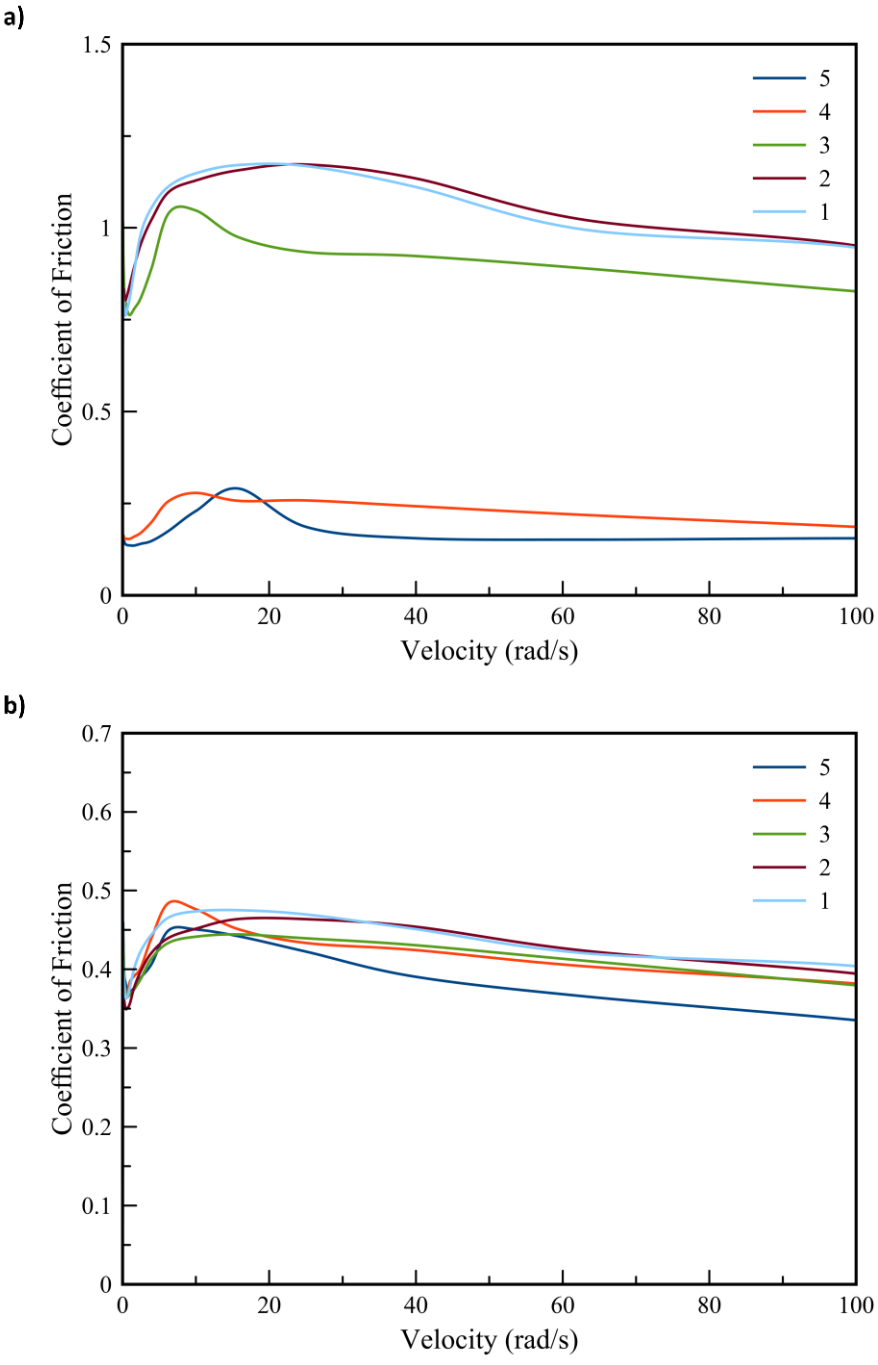

Fig. 23 Friction Coefficient curve with Velocity measured with half ring on plate test of Shea Butter Solid Lipid Nanoparticles at (a) 1N and (b) 3N of each corresponding batch

In Fig. 6b, a similar behavior to that under 3 N is observed since shea butter SLNs with a lower coefficient of friction are the smallest (213 nm). At different normal forces, these nanoparticles have similar behavior, precisely because of the formation of layers on its surface.

All these behaviors are similar to those previously reported for nanoparticles [104], considering having a smaller particle size; improving their lubrication properties, reducing their coefficient of friction and anti-wear property compared to their bulk material [68,105]. Principally due to the formation of nano-films [106].

3.6 Triborheological Testing of Shea Butter SLNs in Evanescent Cream

The triborheology of evanescent cream with SLNs was performed to validate the effect it has on its rheology, further to validate how the amount of SLNs added in the topical formulation affects its lubrication properties. To have a better understanding of how these enhance the properties of the evanescent cream.

Fig. 24a shows that the cream with shea butter SLNs has shear thinning behavior, since it is a colloidal suspension; should the shear rate increases, stress increases due to the interactions of the particles.

In Fig. 24b, the shear thinning behavior is observed as well as the fluid viscosity moves from a higher viscosity at a low shear rate to a lower viscosity at a high shear rate. Furthermore, we can see that at higher concentrations, the viscosity decreased, Being with 15% SLNs the lowest viscosity value. While for low shear rates the highest viscosity is observed at 1% and 2% of SLNs, this is mainly due to a higher concentration of nanoparticles which tend to agglomerate [106–109].

When an axial force of 1 N was applied, the formulations that have shea butter in bulk behave progressively in terms of their COF, while those with SLNs decrease to a certain percentage, with 2.5% of shea butter SLNs, and then increases its COF (Fig. 25). Consequently SLNs at higher quantities tend to agglomerate due to their proximity between them and their high surface energy [110,111].

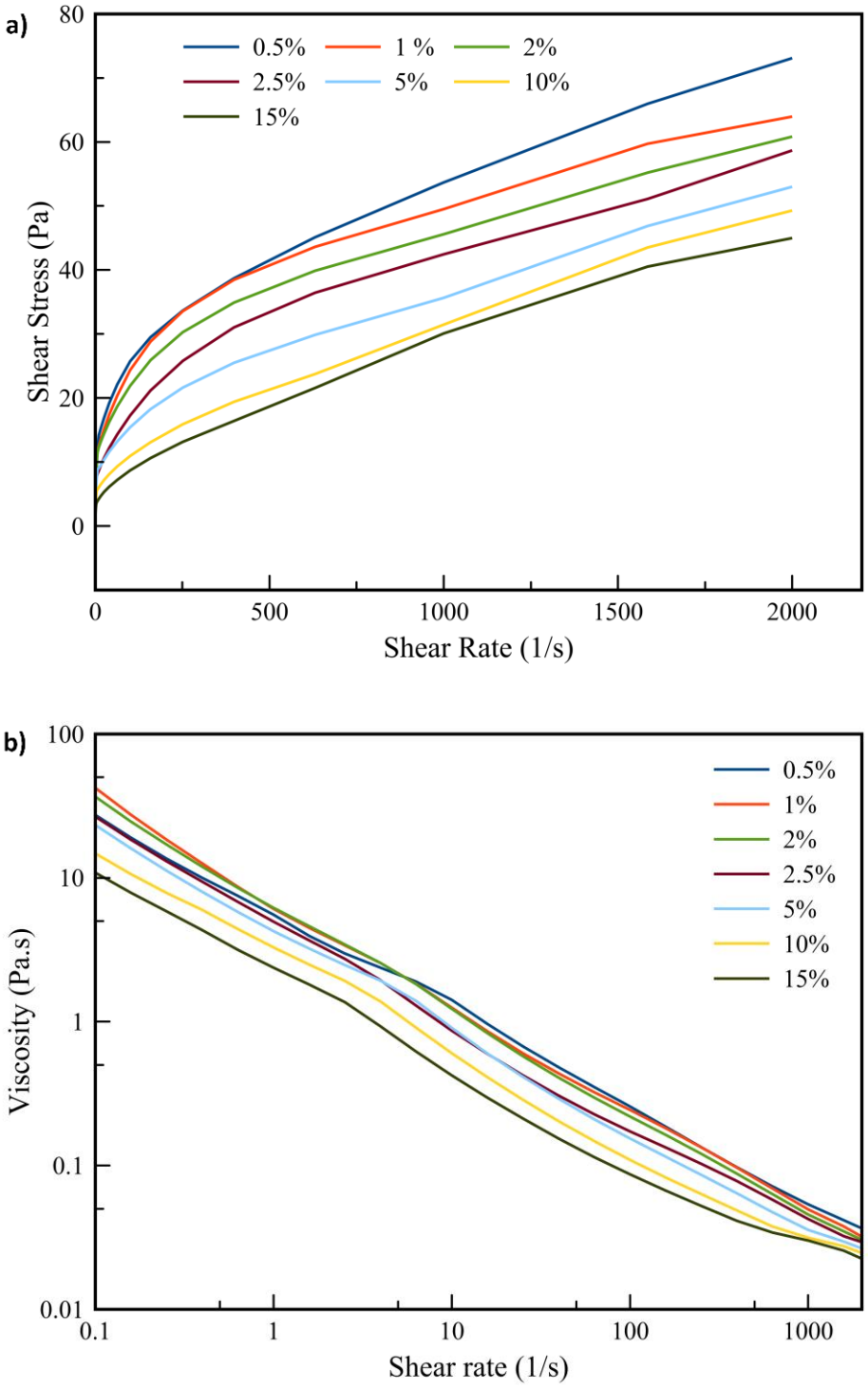

Fig. 24 (a) Shear Stress against shear rate and (b) Comparison of Viscosity with the Shear rate for Evanescent Cream with Shea Butter SLNs (213 nm) at different concentrations

It is also observed that the one with the highest COF is the formulation which has 0.5% shea butter in bulk, while the one with the lowest COF is the formulation with 2.5% shea butter SLNs.

While at 3 N the topical formulation which has better lubrication properties are those having 0.5% of shea butter SLNs and the one with a higher COF 1-2% of shea butter bulk. Similar to the previous 1 N test, increasing its COF to a higher amount of shea butter SLNs and with greater amount of shea butter bulk its COF decreases.

Essentially this occurs because nanoparticles have a smaller size than bulk materials, allowing to reduce the surface roughness and lower the coefficient of friction, however but when it has a higher number of nanoparticles they tend to agglomerate and begin to form jagged layers on the surface; thus, the coefficient of friction is lower whereas that in bulk but greater than such of a moderate amount of SLNs [63].

It can be observed that at 3N at low speeds has an inverse behavior concerning viscosity, obtaining the highest COF value with the highest percentage of SLNs, while the lowest COF value has the lowest percentage of nanoparticles. Therefore, the one with the highest viscosity, at a medium shear rate, would be the one with the lowest COF, at low speeds at 3N, Fig. 24b and Fig. 24b.

The relationship with tribology at 1N is the value which has the lowest COF at medium and high speeds (2.5% SLNs), this concentration of SLNs is the one that has a medium viscosity at medium to high shear rates, which means that we consider the topical cream is applied at an axial force of 1N and at medium speed. Here, the topical cream that would be easier to apply and may form a more protective layer being the one with 2.5%, due to its medium viscosity and low COF.

Table 2. Triborheological properties of Topical cream with shea butter SLNs

Topical cream with shea butter SLNs (%)	*Zero Shear Viscosity (Pa)*	*Zero Shear Stress (Pa.s)*	*COF at 10 rad/s, 1N*	*COF at 100 rad/s, 1N*
0.5	262.119 ± 1.23	2.62763 ± 0.05	0.72756 ± 0.1	0.56690 ± 0.012
1	441.409 ± 1.12	4.42108 ± 0.03	0.63221 ± 0.09	0.53753 ± 0.013
2	299.629 ± 1.05	3.00216 ± 0.04	0.6334 ± 0.07	0.46219 ± 0.011
2.5	**219.277 ± 1.06**	**2.1953 ± 0.08**	**0.61712 ± 0.05**	**0.35632 ± 0.012**
5	207.525 ± 1.15	2.0797 ± 0.09	0.69517 ± 0.06	0.45681 ± 0.013
10	105.488 ± 1.34	1.0563 ± 0.02	0.76381 ± 0.08	0.79167 ± 0.022
15	71.9537 ± 1.45	0.72064 ± 0.04	0.765517 ± 0.1	0.72471 ± 0.015

In Table 2. we can observe a comparison between the topical cream with shea butter SLNs at different percentages. It is validated that the lowest COF at low and high speeds is with 2.5% of nanoparticles, we also have a medium viscosity that gives us a stable cream and will give us excellent penetration properties, obtaining uniformity of this cream on the skin.

It must be taken into account that creams which also have a silky feel are those which have lower coefficients of friction at low speeds, meaning that although in some cases SLNs have a final coefficient of friction equal to or greater than bulk lipid formulations, all SLNs formulations at low speeds have a lower coefficient of friction, indicating that they have a more silky feel than those composed of bulk lipids [70].

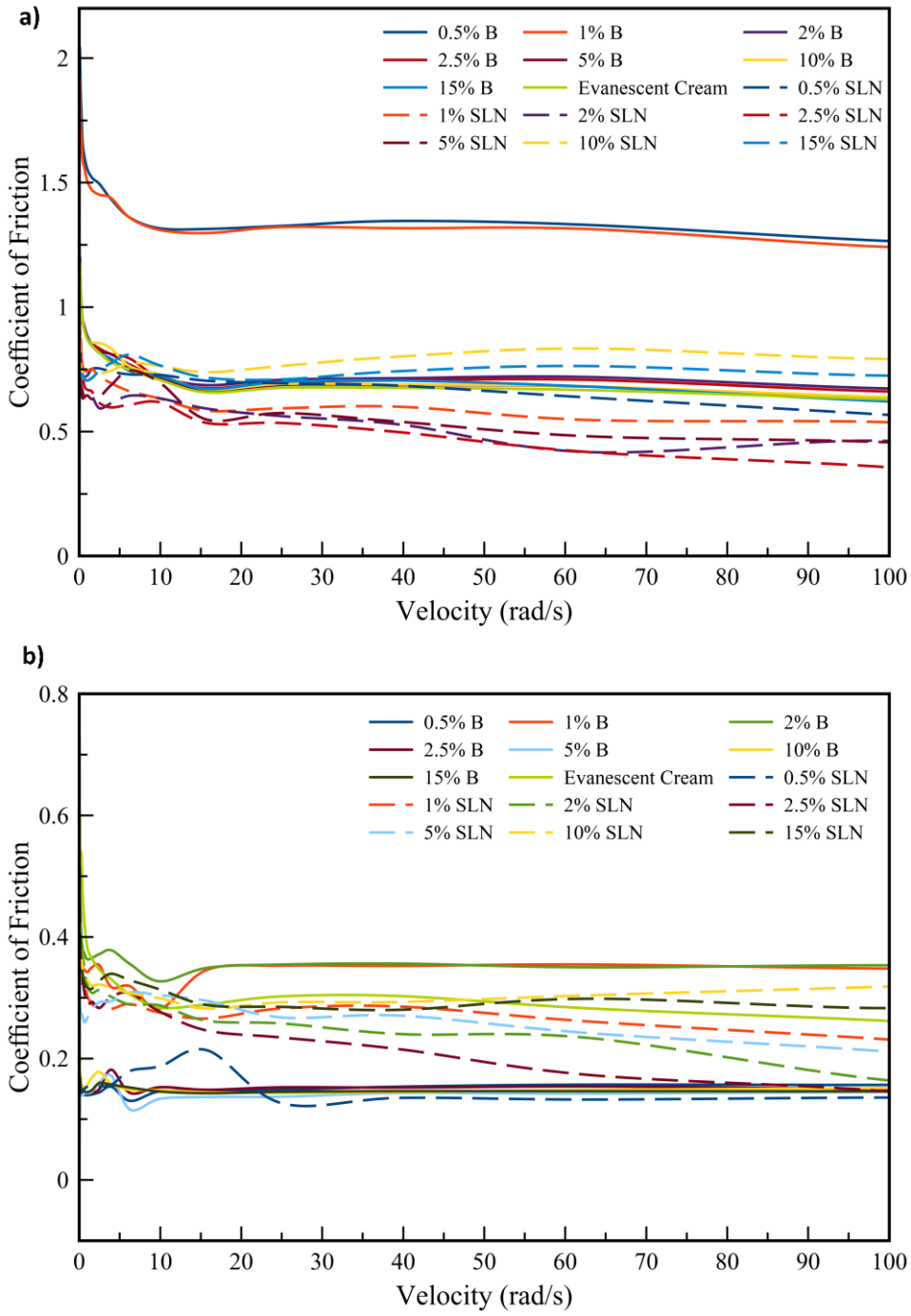

Fig. 25 Friction Coefficient curve with Velocity measured with half ring on plate test of Shea Butter Solid Lipid Nanoparticles (213 nm) and Bulk Shea Butter at (a) 1N and (b) 3N

In Fig. 25, behaviors dissimilar to a normal Stribeck´s curve can be observed due to the generation of lipid layers on the surface. These layers are growing

roughly, and as the speed increases these layers cause a raise in the coefficient of friction owing to their irregularity; as the speed increases, a homogeneous layer is re-formed on the surface.

This behavior is visible when grease lubricants are used because shea butter has fat formed by lipids, which easily tend to form layers on the surface, Fig. 20C [112]. For this reason, the lubrication mechanism of the SLNs is with a protective film (Fig. 26), being when the nanoparticles form a lubricating layer (physical film) on the surface, reducing the contact area [67,113,114]. Increasing the lubricating properties of the topical formulation, resulting in greater occlusion, hydration, protection against external agents, reduction of skin irritation, and high emolliency.

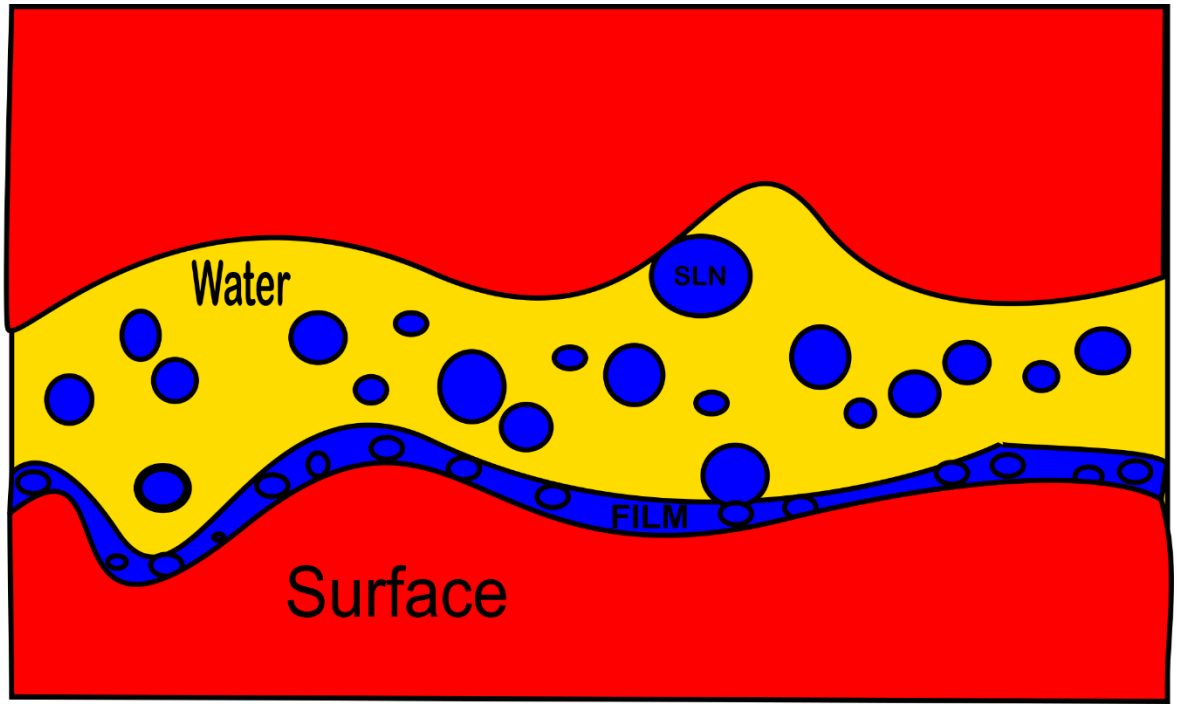

Fig. 26 Lubrication mechanism of Shea Butter SLNs, protective film

3.7 Biotriborheology of Shea Butter SLNs

To prove the penetration of SLNs through the skin and the occlusive/moisture effect of topical cream with SLNs, studies of biotriborheology, and confocal microscopy were conducted.

At 0.2 N, the cream with the lowest coefficient of friction was that with 0.5% shea butter SLNs and the highest coefficient of friction was that with 15% shea butter SLNs (Fig. 27a).

At 1 N, it can be seen that formulations with SLNs at low speeds have a higher coefficient of friction than such of bulk shea butter, this is principally due to at low speeds, the higher COFs in biotribology are related to greater hydration in the skin [60,115]; the one with the lowest COF is that with an SLNs percentage of 10%, whereas the highest COF is the one which involves 2% of bulk shea butter at medium and higher speeds (Fig. 27b).

The formulation with 5% shea butter SLNs possesses the lowest coefficient of friction, and 2 % SLNs shea butter at 3 N has the highest coefficient of friction (Fig. 27c). It can be seen that they have different behavior than the aluminum surface because SLNs penetrate the skin. Although the decrease of COF and the formation of a homogeneous layer were not completely achieved, in all three cases, shea butter SLNs had the coefficient of friction lower than those of the bulk lipid.

Table 3. Biotriborheological studies of Topical cream with SLNs and raw shea butter

	Raw shea butter		***Shea butter SLNs***	
Topical cream (%)	**COF at 10 rad/s, 1N**	**COF at 100 rad/s, 1N**	**COF at 10 rad/s, 1N**	**COF at 100 rad/s, 1N**
0.5	1.1308 ± 0.03	0.8063 ± 0.012	1.0587 ± 0.04	0.71832 ± 0.012
1	1.06767 ± 0.05	0.8101 ± 0.014	0.96671 ± 0.04	0.71187 ± 0.011
2	1.22994 ± 0.01	0.8868 ± 0.019	1.16935 ± 0.07	0.81111 ± 0.016
2.5	**1.25183 ± 0.02**	0.8696 ± 0.014	**1.25944** ± 0.02	0.73919 ± 0.016
5	1.20948 ± 0.04	0.8853 ± 0.011	1.25393 ± 0.05	0.80593 ± 0.027
10	1.15940 ± 0.02	0.8273 ± 0.013	0.83625 ± 0.01	**0.60444 ± 0.022**
15	1.10328 ± 0.03	**0.7503 ± 0.014**	1.09928 ± 0.01	0.85877 ± 0.024

Table 3. shows that the highest COF among all topical creams at low speeds were with SLNs 2.5% shea butter topical cream, which best moisturizes the skin. At the same time, we can observe that the lowest COF at high speeds was 10% of the SLN of shea butter, which indicates that there is penetration into the skin that follows in an irregular formation of lipid layers in the skin, therefore does not exist a relationship in the COFs. at high speeds.

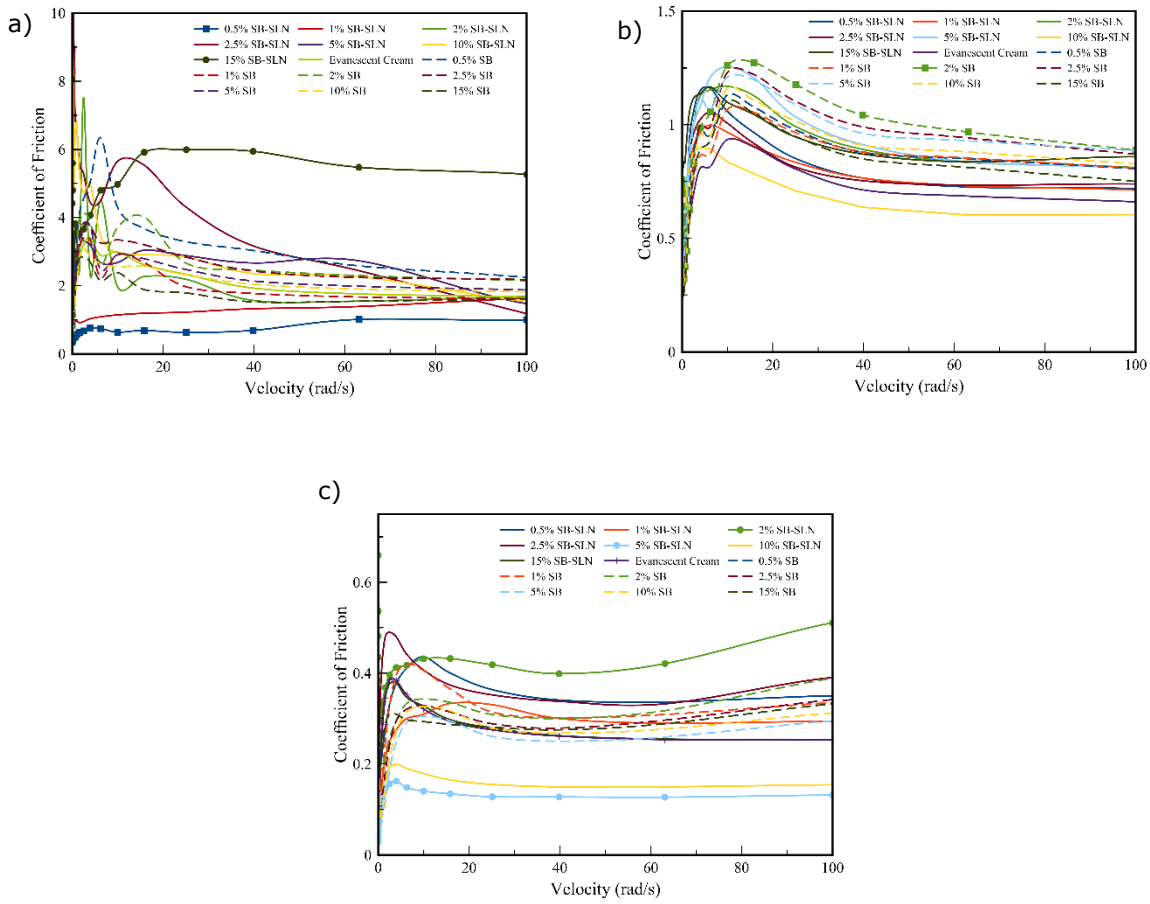

Fig. 27 Friction Coefficient curve with Velocity measured with half ring on porcine skin test of Shea Butter Solid Lipid Nanoparticles (213 nm) and Bulk Shea Butter at (a) 0.2N, (b) 1N and (c) 3N

3.6.1 Confocal Analysis

In Fig. 28 it can be confirmed that shea butter SLNs are fluorescent in coumarin- 6 green color, and that porcine skin does not exhibit any kind of fluorescent effect in this wavelength, also we can confirm the increase of the fluorescence effect of the nanoparticles.

Performing Z-stack from 0 nm to 10 µm, with 2.5 µm slide-cuts, considering that the maximum thickness of porcine skin that would be observed is 10 µm. It can be seen that the decrease in coumarin-6 green color indicates less number of nanoparticles, meaning reduced penetration, according to this study the penetration was successful up to 10 µm if there is the same number of nanoparticles included in

each layer. Furthermore, the formation of layers in the skin can be observed through these confocal images, as confirmed in Fig. 20C. In response to this, it is seen that with the Franz cells at 25 min, there is a penetration of up to 10 μm. By using an axial force, those at 20 min can be compared with a force of 0.2 N, 15 min with a force of 1 N and at 10 min with a force of 3 N, as shown in Fig. 29. It is observed that the longer the exposure time, the fluorescence increases for all SLN samples [116–118].

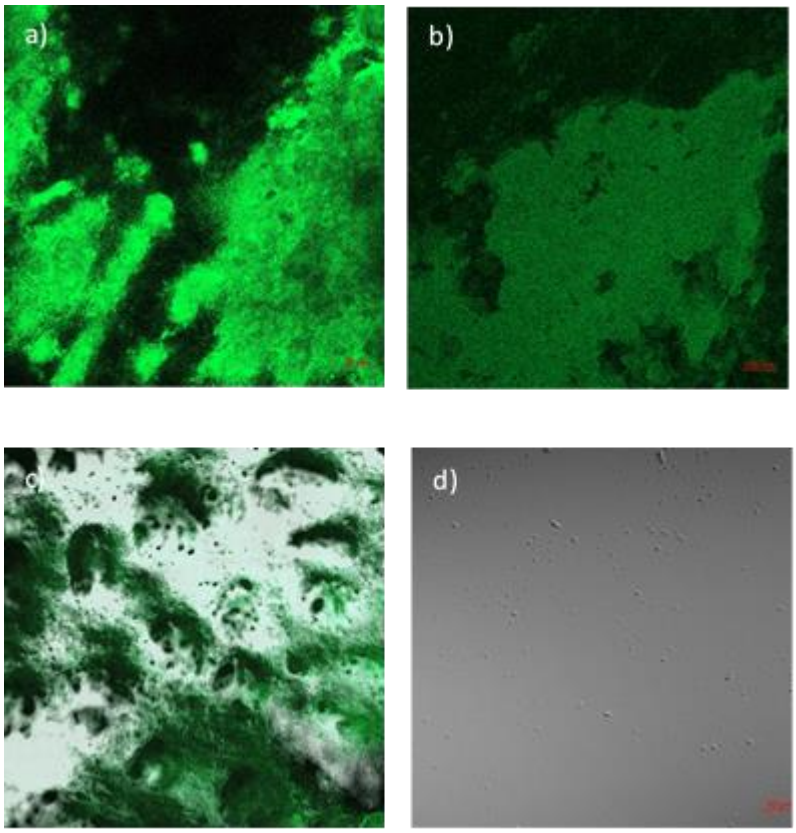

Fig. 28 Confocal microscopy images a) shea butter SLNs in porcine skin, b) bulk shea butter, c) contrast of shea butter SLNs with porcine skin and d) porcine skin.

In Fig. 30. Stribeck curves of shea butter SLNs in porcine skin are shown, observing that greater axial force the coefficient of friction decreases, additionally at 1 N and 3 N at 15 and 10 minutes respectively, both have an intermediate COF, due to the penetration of the SLNs and the formation of the lipid layer, but at 0.2 N it is observed that at 20 minutes, which is the greatest penetration, it has the highest COF, this is due to the irregular formation of lipid layer on the skin, in

contradistinction to 1 N and 3 N, which has a more homogeneous formation of this layer, similar behavior to the previous ones.

In the literature, it is found that the smaller the mean particle size, the more reliable the penetration of the SLNs [86,119–123]. Additionally, by exerting a greater axial force, it is deduced that these nanoparticles penetrate in less time. It is also shown that when an axial force (1 N) is exerted on the skin with SLNs, results in a better distribution of the nanoparticles, but if we exert a force of 3 N, this distribution concentrates in certain grooves depending on the geometry. For this reason it is inferred that the best application force is at 1 N

Through the penetration of the shea butter SLNs, it is deduced that the biotriborheology graphs are different from the triborheology graphs due to the formation of inhomogeneous lipid layers, as in the case of triborheology, forming unequal layers due to the axial force. It should be noted that this is the first time that the triborheology study of SLNs is carried out on porcine skin (biotriborheology) and how the force exerted affects on them was evaluated. In the same way, the biotriborheology of the SLNs in base cream is a new study. A diagram of the proposed biotriborheology system can be visualized in Fig. 13.

a

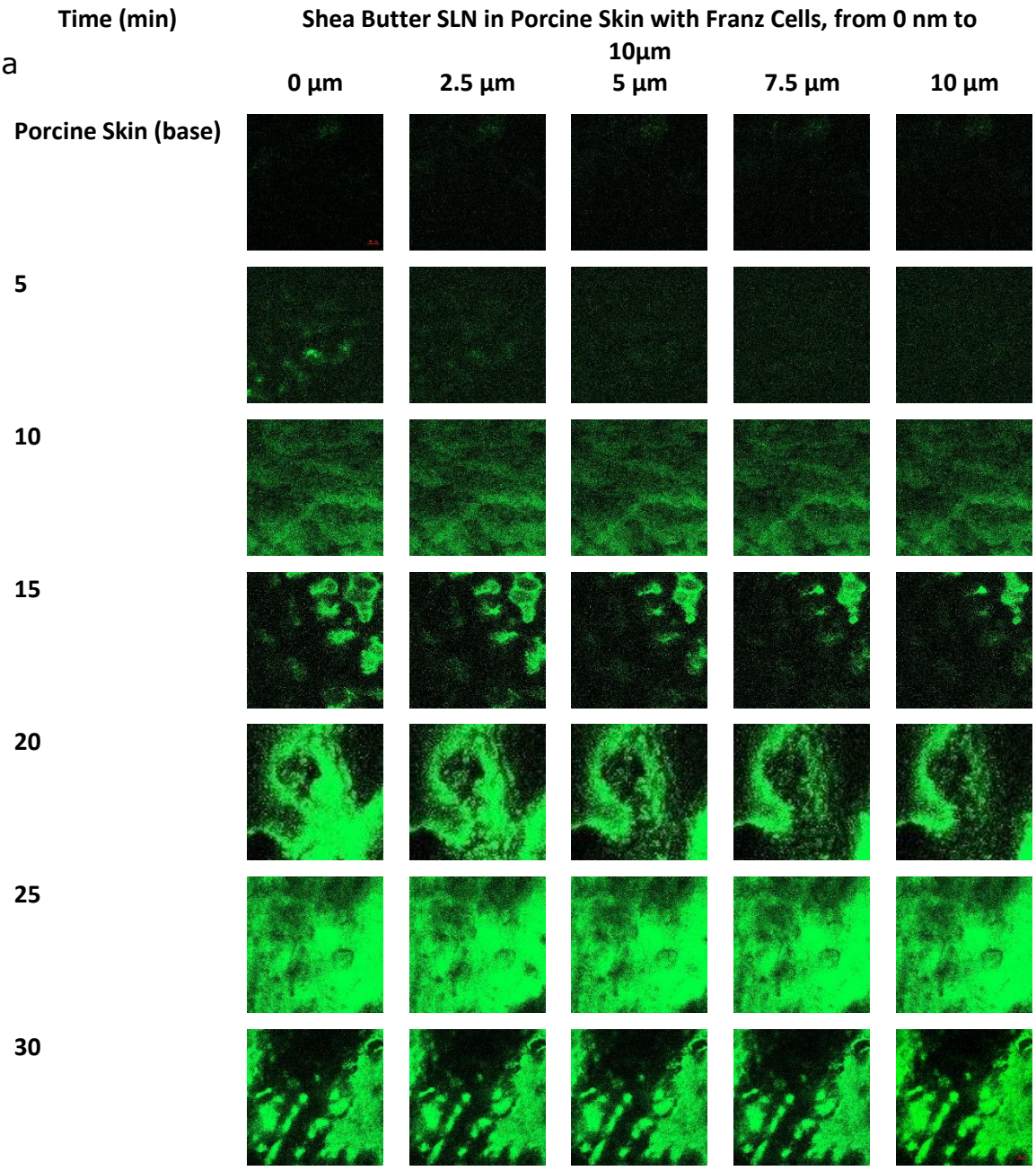
Time (min)
Shea Butter SLN in Porcine Skin with Franz Cells, from 0 nm to 10µm
0 µm
2.5 µm
5 µm
7.5 µm
10 µm
Porcine Skin (base)
5
10
15
20
25
30

b

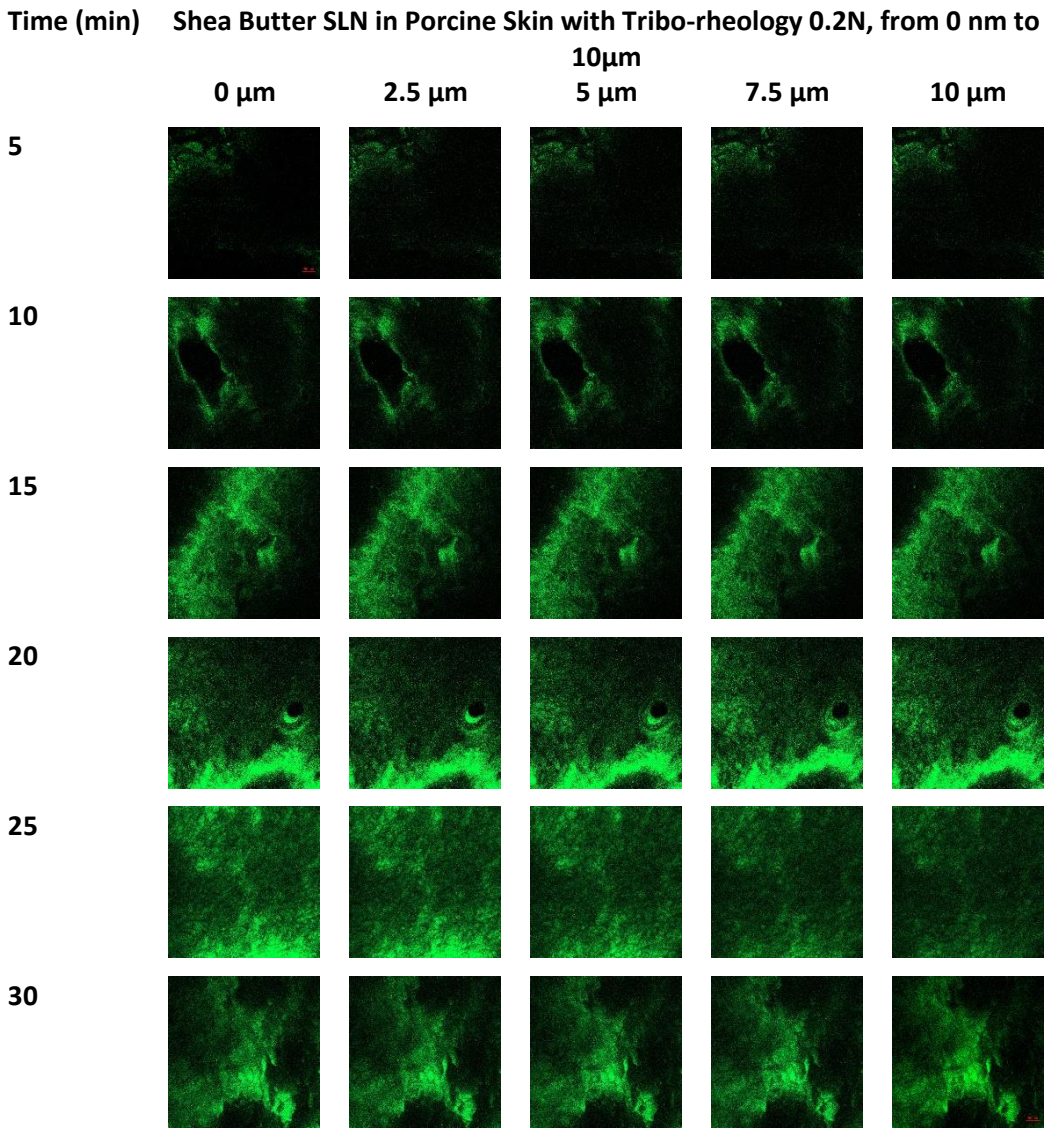
Time (min)
Shea Butter SLN in Porcine Skin with Tribo-rheology 0.2N, from 0 nm to 10µm
0 µm
2.5 µm
5 µm
7.5 µm
10 µm
5
10
15
20
25
30

C

Time (min)	Shea Butter SLN in Porcine Skin with Tribo-rheology 1N, from 0 nm to 10µm				
	0 µm	2.5 µm	5 µm	7.5 µm	10 µm
5	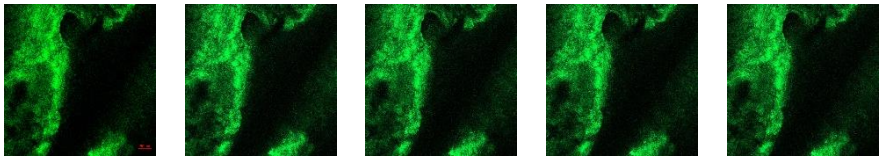				
10	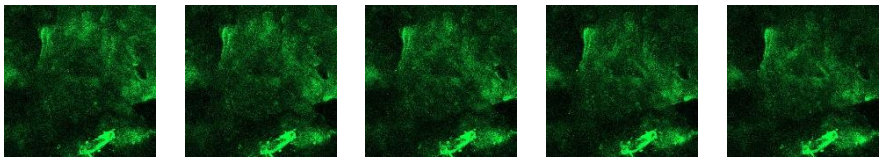				
15	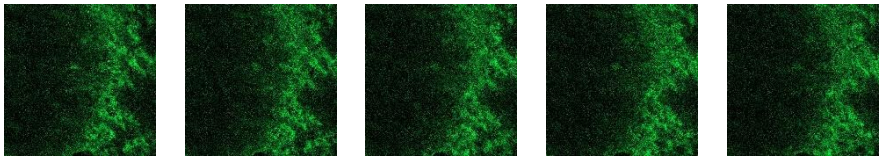				
20	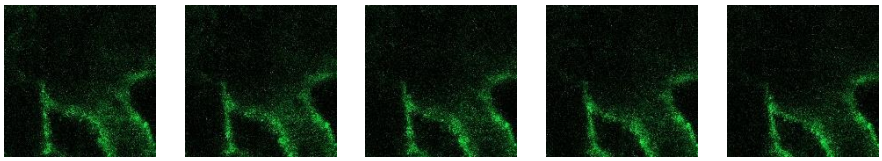				
25	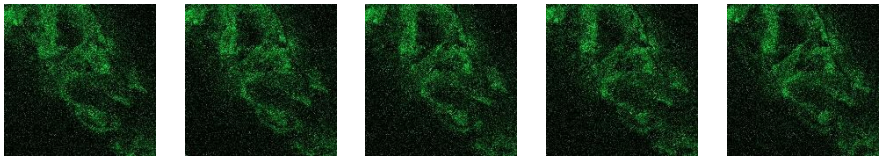				
30	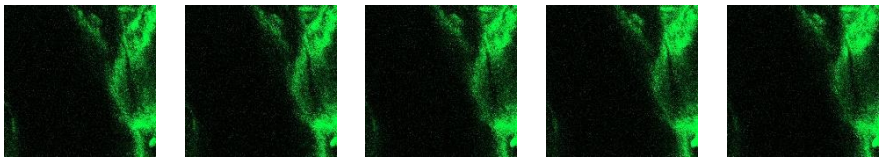				

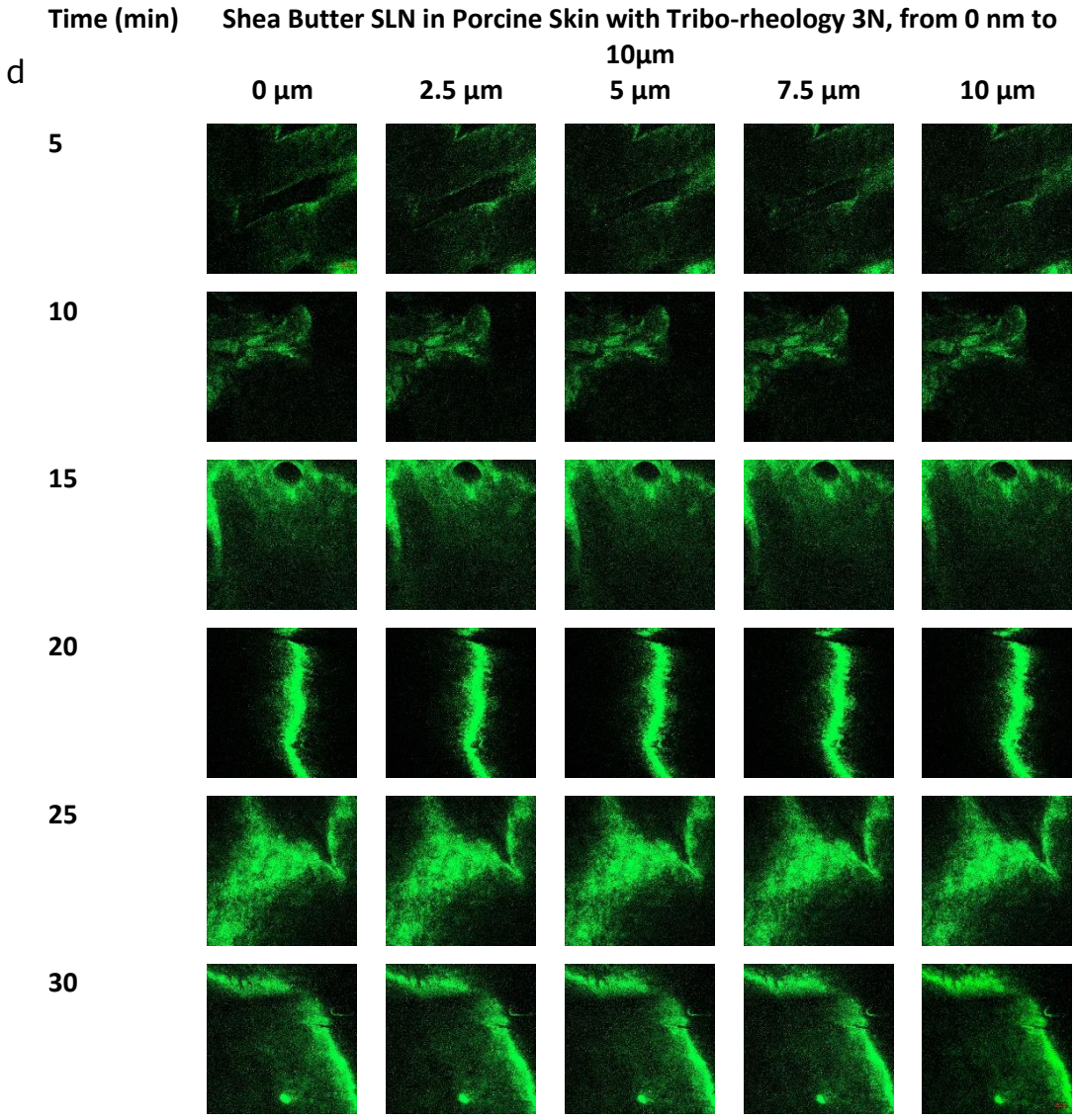

Fig. 29 Penetration of Shea Butter SLNs (green coumarin) at several times with Confocal Images in Porcine Skin a) Franz Cells (0N) and Tribology at b)0.2N c)1N and d) 3N

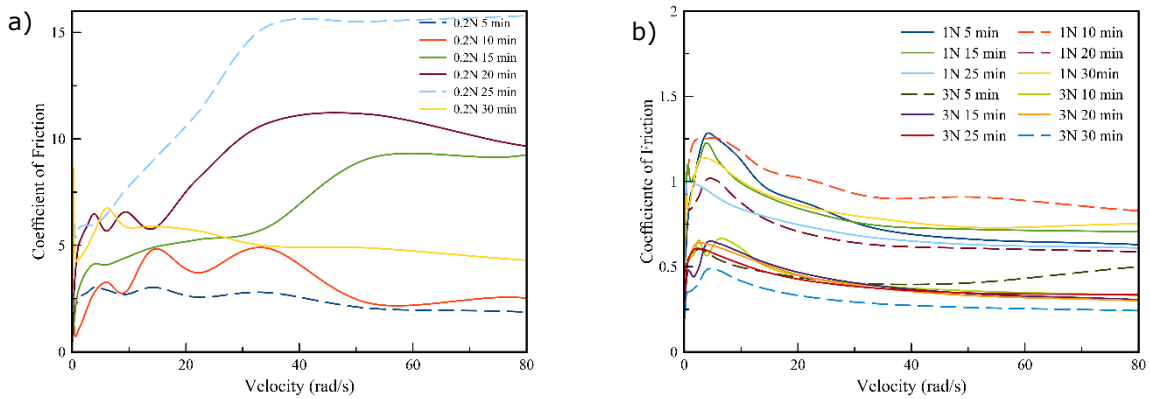

Fig. 30 Friction Coefficient curve with Velocity measured with half ring on porcine skin test of Shea Butter Solid Lipid Nanoparticles (213 nm) for 5 min to 30 min at different axial forces

Chapter 4

Conclusions

SLNs of a size of approximately 220 nm were obtained. A round and smooth shape is confirmed by SEM and AFM. The stability of the nanoparticles was confirmed, since the SLNs did not increase in size for a month, and after 3 months, they did not grow significantly.

From the triborheological studies, it was obtained that the formulation which has the lowest COF at 1 N is 2.5% SLNs (w/w) and for 3 N, it is 0.5% SLNs (w/w); this is mainly because nanoparticles having a smaller particle size allow them to adhere better to the surface, creating a more homogeneous layer, which reduces friction (protective film mechanism). Nevertheless, should more SLNs be added, they agglomerate and begin to increase in size, obtaining a COF similar to the formulations without SLNs.

The penetration of SLNs can be confirmed due to biotriborheology and confocal microscopy. During penetration, the layers in the skin are not formed in the same way, producing a different behavior than having an aluminum surface, due to the layer of the lipid generates not homogenously, as it is in the case of the triborheology that the behavior was obtained of the formation of these lipid layers, which is better explained. Moreover, the best axial force to have a better distribution of SLNs is 1 N, which can enhance penetration. Furthermore, the impact that SLNs have on topical formulations is confirmed, since they improve penetration, have better occlusion and allow the formation of smaller lipid layers, producing a reduction in the COF, better lubrication properties related to enhancement in hydration, occlusion and emollient effect .

Bibliography

[1] **Haque S, Whittaker M, Mcintosh MP, Pouton CW, Phipps S, Kaminskas LM. A comparison of the lung clearance kinetics of solid lipid nanoparticles and liposomes by following the 3 H-labelled structural lipids after pulmonary delivery in rats. Eur J Pharm Biopharm 2018;125:1–12. doi:10.1016/j.ejpb.2018.01.001.**

[2] **Saloni, Khogta; Jahanvi, Patel; Kalyani, Barve; Vaishali L. Herbal Nano-formulations for Topical Delivery. J Herb Med 2019. doi:10.1016/j.neubiorev.2019.07.019.**

[3] **Nakasato, Daniele; Pereira, Anderson; Oliveira J. Evaluation of the effects of polymeric chitosan/tripolyphosphate and solid lipid nanoparticles on germination of Zea mays, Brassica rapa and Pisum sativum. Ecotoxicol Environ Saf 2017;142:369–74. doi:10.1016/j.ecoenv.2010.08.031.**

[4] **Flores FC, Paese K, Weber J, Antunes JB, Pohlmann AR, Guterres SS, et al. Lipid Nanoparticles Obtained with Innovative Natural Materials for Topical Delivery of Tioconazole: Mangospheres. J Nanosci Nanotechnol 2017;17:1762–70. doi:10.1166/jnn.2017.13019.**

[5] **Pham DTTT, Tran PHLL, Tran TTDD. Development of solid dispersion lipid nanoparticles for improving skin delivery. Saudi Pharm J 2019;27:1019–24. doi:10.1016/j.jsps.2019.08.004.**

[6] **Zhong Q, Zhang L. Nanoparticles fabricated from bulk solid lipids: Preparation, properties, and potential food applications. Adv Colloid Interface Sci 2019;273:102033. doi:10.1016/j.cis.2019.102033.**

[7] **Rigano L, Lionetti N. Nanobiomaterials in galenic formulations and cosmetics. In: Grumezescu A, editor. Nanobiomaterials Galen. Formul. Cosmet. Appl. Nanobiomaterials. 1st ed., Bucharest, Romania: Elsevier; 2016, p. 121–48.**

[8] **Ganesan P, Narayanasamy D. Lipid nanoparticles: Different preparation**

techniques, characterization, hurdles, and strategies for the production of solid lipid nanoparticles and nanostructured lipid carriers for oral drug delivery. Sustain Chem Pharm 2017;6:37–56. doi:10.1016/j.scp.2017.07.002.

[9] Marin, Retamal; Babick, F.; Hillemann L. Zeta potential measurements for non-spherical colloidal particles – Practical issues of characterisation of interfacial properties of nanoparticles. Colloids Surfaces A 2017;532. doi:10.1016/j.colsurfa.2017.04.010.

[10] Peng TX, Liang DS, Guo F, Peng H, Xu YC, Luo NP, et al. Enhanced storage stability of solid lipid nanoparticles by surface modification of comb-shaped amphiphilic inulin derivatives. Colloids Surfaces B Biointerfaces 2019;181:369–78. doi:10.1016/j.colsurfb.2019.05.061.

[11] Gordillo-Galeano A, Mora-Huertas CE. Solid lipid nanoparticles and nanostructured lipid carriers: A review emphasizing on particle structure and drug release. Eur J Pharm Biopharm 2018;133:285–308. doi:10.1016/j.ejpb.2018.10.017.

[12] Varenne F, Hillaireau H, Bataille J, Smadja C, Barratt G, Vauthier C. Application of validated protocols to characterize size and zeta potential of dispersed materials using light scattering methods. Colloids Surfaces A Physicochem Eng Asp 2019;560:418–25. doi:10.1016/J.COLSURFA.2018.09.006.

[13] Lorenzen, Ana; Rossi, Thais; Riegel-Vidotti, Izabel; Vidotti M. Influence of cationic and anionic micelles in the (sono)chemical synthesis of stable Ni(OH)2 nanoparticles: "In situ" zeta-potential measurements and electrochemical properties. Appl Surf Sci 2018;455:357–66. doi:10.1016/j.apsusc.2018.05.198.

[14] Hanaor, Dorian; Michelazzi, Marco; Leonelli, Cristina; Sorrel C. The effects of carboxylic acids on the aqueous dispersion and electrophoretic deposition of ZrO2. J Eur Ceram Soc 2012;32:235–44. doi:10.1016/j.jeurceramsoc.2011.08.015.

[15] Paredes Salido F, Roca Fernández JJ. Influencia de los radicales libres en el

envejecimiento celular. Offarm 2002;21:96–100.

[16] Morteza-Semnani K, Akbari J, Nokhodchi A, Rostamkalaei SS, Saeedi M. Topical gel of Metformin solid lipid nanoparticles: A hopeful promise as a dermal delivery system. Colloids Surfaces B Biointerfaces 2018;175:150–7. doi:10.1016/j.colsurfb.2018.11.072.

[17] Ravanfar R, Tamaddon AM, Niakousari M, Moein MR. Preservation of anthocyanins in solid lipid nanoparticles: Optimization of a microemulsion dilution method using the Placket-Burman and Box-Behnken designs. Food Chem 2016;199:573–80. doi:10.1016/j.foodchem.2015.12.061.

[18] Shakeri M, Razavi SH, Shakeri S. Carvacrol and astaxanthin co-entrapment in beeswax solid lipid nanoparticles as an efficient nano-system with dual antioxidant and anti-biofilm activities. Lwt 2019;107:280–90. doi:10.1016/j.lwt.2019.03.031.

[19] Villalobos-Hernández JR, Müller-Goymann CC. Sun protection enhancement of titanium dioxide crystals by the use of carnauba wax nanoparticles: The synergistic interaction between organic and inorganic sunscreens at nanoscale. Int J Pharm 2006;322:161–70. doi:10.1016/j.ijpharm.2006.05.037.

[20] Shtay R, Keppler JK, Schrader K, Schwarz K. Encapsulation of (−)-epigallocatechin-3-gallate (EGCG) in solid lipid nanoparticles for food applications. J Food Eng 2019;244:91–100. doi:10.1016/j.jfoodeng.2018.09.008.

[21] Garti N, Widlak NR. Cocoa Butter and Related Compounds. Elsevier Inc.; 2012. doi:10.1016/C2015-0-02409-1.

[22] Lovett PN. Shea butter: Properties and processing for use in food. Spec. Oils Fats Food Nutr. Prop. Process. Appl., 2015, p. 125–58. doi:10.1016/C2014-0-01770-4.

[23] Abdel-Aal1 HA, Zahouani H, Mansori M El. A comparative Study of Frictional Response of Shed Snakeskin and Human Skin. Wear 2017;377:281–94. doi:10.1016/j.wear.2016.12.055.

[24] Garcês A, Amaral MH, Sousa Lobo JM, Silva AC. Formulations based on solid lipid nanoparticles (SLN) and nanostructured lipid carriers (NLC) for cutaneous use: A review. Eur J Pharm Sci 2018;112:159–67. doi:10.1016/j.ejps.2017.11.023.

[25] Hadidi M, Pouramin S, Adinepour F, Haghani S, Jafari SM. Chitosan nanoparticles loaded with clove essential oil: Characterization, antioxidant and antibacterial activities. Carbohydr Polym 2020;236:116075. doi:10.1016/j.carbpol.2020.116075.

[26] Schwingen J, Kaplan M, Kurschus FC. Review—current concepts in inflammatory skin diseases evolved by transcriptome analysis: In-depth analysis of atopic dermatitis and psoriasis. Int J Mol Sci 2020;21. doi:10.3390/ijms21030699.

[27] de Carvalho SM, Noronha CM, da Rosa CG, Sganzerla WG, Bellettini IC, Nunes MR, et al. PVA antioxidant nanocomposite films functionalized with alpha-tocopherol loaded solid lipid nanoparticles. Colloids Surfaces A Physicochem Eng Asp 2019;581:123793. doi:10.1016/j.colsurfa.2019.123793.

[28] Gore E, Picard C, Savary G. Spreading behavior of cosmetic emulsions: Impact of the oil phase. Biotribology 2018;16:17–24. doi:10.1016/j.biotri.2018.09.003.

[29] Burke KE. Prevention and Treatment of Aging Skin with Topical Antioxidants. Ski. Aging Handb., Elsevier Inc.; 2009, p. 149–76. doi:10.1016/B978-0-8155-1584-5.50012-0.

[30] Karuppagounder V, Nomoto M, Watanabe K. Antiinflammatory Effects of Kampo Medicines in Atopic Dermatitis. Japanese Kampo Med. Treat. Common Dis. Focus Inflamm., Elsevier; 2017, p. 89–95. doi:10.1016/B978-0-12-809398-6.00010-X.

[31] HORAN JD, HUDSON AL. Atopic dermatitis (eczema). Can Med Assoc J 1963;88:45–6. doi:10.1016/b978-0-7020-5514-0.00018-x.

[32] Maarouf M, Tran K, Yozwiak M, Sligh J, Wondrak G, Shi V. 664 Atopic

dermatitis: Linking skin barrier function with antioxidant defense. J Invest Dermatol 2018;138:S113. doi:10.1016/j.jid.2018.03.673.

[33] Wu X, Zhang H, He S, Yu Q, Lu Y, Wu W, et al. Improving dermal delivery of hyaluronic acid by ionic liquids for attenuating skin dehydration. Int J Biol Macromol 2020;150:528–35. doi:10.1016/j.ijbiomac.2020.02.072.

[34] Abdel-Mottaleb MMA. Nanoparticles for Treatment of Atopic Dermatitis. Nanosci. Dermatology, Elsevier Inc.; 2016, p. 167–75. doi:10.1016/B978-0-12-802926-8.00013-6.

[35] Miyahara R. Emollients. Cosmet. Sci. Technol. Theor. Princ. Appl., Elsevier Inc.; 2017, p. 245–53. doi:10.1016/B978-0-12-802005-0.00016-1.

[36] Sidbury R. Newborn Skin Development: Structure and Function. Avery's Dis. Newborn Tenth Ed., Elsevier Inc.; 2018, p. 1468-1474.e1. doi:10.1016/B978-0-323-40139-5.00103-0.

[37] Bakowska-Barczak A, Larminat MA de, Kolodziejczyk PP. The application of flax and hempseed in food, nutraceutical and personal care products. Handb. Nat. Fibres Vol. 2 Process. Appl., Elsevier Inc.; 2020, p. 557–90. doi:10.1016/B978-0-12-818782-1.00017-1.

[38] Boguniewicz M, Fonacier L, Leung DYM. Atopic and Contact Dermatitis. Clin. Immunol., Elsevier; 2019, p. 611-624.e1. doi:10.1016/B978-0-7020-6896-6.00044-2.

[39] Wiesenthal A, Hunter L, Wang S, Wickliffe J, Wilkerson M. Nanoparticles: Small and mighty. Int J Dermatol 2011;50:247–54. doi:10.1111/j.1365-4632.2010.04815.x.

[40] Puglia C, Bonina F. Lipid nanoparticles as novel delivery systems for cosmetics and dermal pharmaceuticals. Expert Opin Drug Deliv 2012;9:429–41. doi:10.1517/17425247.2012.666967.

[41] Gloor M. How do dermatological vehicles influence the horny layer? Skin Pharmacol Physiol 2004;17:267–73. doi:10.1159/000081111.

[42] Keck CM, Schwabe K. Silver-nanolipid complex for application to atopic dermatitis skin: Rheological characterization, in vivo efficiency and theory of action. J Biomed Nanotechnol 2009;5:428–36. doi:10.1166/jbn.2009.1053.

[43] Damiani G, Eggenhöffner R, Pigatto PDM, Bragazzi NL. Nanotechnology meets atopic dermatitis: Current solutions, challenges and future prospects. Insights and implications from a systematic review of the literature. Bioact Mater 2019;4:380–6. doi:10.1016/j.bioactmat.2019.11.003.

[44] Rujido-Santos I, Naveiro-Seijo L, Herbello-Hermelo P, Barciela-Alonso M del C, Bermejo-Barrera P, Moreda-Piñeiro A. Silver nanoparticles assessment in moisturizing creams by ultrasound assisted extraction followed by sp-ICP-MS. Talanta 2019;197:530–8. doi:10.1016/j.talanta.2019.01.068.

[45] Bianco C, Visser MJ, Pluut OA, Svetličić V, Pletikapić G, Jakasa I, et al. Characterization of silver particles in the stratum corneum of healthy subjects and atopic dermatitis patients dermally exposed to a silver-containing garment. Nanotoxicology 2016;10:1480–91. doi:10.1080/17435390.2016.1235739.

[46] Pandey M, Choudhury H, Gunasegaran TAP, Nathan SS, Md S, Gorain B, et al. Hyaluronic acid-modified betamethasone encapsulated polymeric nanoparticles: fabrication, characterisation, in vitro release kinetics, and dermal targeting. Drug Deliv Transl Res 2019;9:520–33. doi:10.1007/s13346-018-0480-1.

[47] Sandri G, Bonferoni MC, Gkçe EH, Ferrari F, Rossi S, Patrini M, et al. Chitosan-associated SLN: In vitro and ex vivo characterization of cyclosporine A loaded ophthalmic systems. J Microencapsul 2010;27:735–46. doi:10.3109/02652048.2010.517854.

[48] Kang J-H, Chon J, Kim Y-I, Lee H-J, Oh D-W, Lee H-G, et al. Preparation and evaluation of tacrolimus-loaded thermosensitive solid lipid nanoparticles for improved dermal distribution. Int J Nanomedicine 2019;Volume 14:5381–96. doi:10.2147/IJN.S215153.

[49] Singh KK, Pople P. Safer than safe: Lipid nanoparticulate encapsulation of

tacrolimus with enhanced targeting and improved safety for atopic dermatitis. J Biomed Nanotechnol 2011;7:40–1. doi:10.1166/jbn.2011.1191.

[50] Pople P V., Singh KK. Development and evaluation of colloidal modified nanolipid carrier: Application to topical delivery of tacrolimus. Eur J Pharm Biopharm 2011;79:82–94. doi:10.1016/j.ejpb.2011.02.016.

[51] Siddique MI, Katas H, Iqbal Mohd Amin MC, Ng SF, Zulfakar MH, Buang F, et al. Minimization of Local and Systemic Adverse Effects of Topical Glucocorticoids by Nanoencapsulation: In Vivo Safety of Hydrocortisone-Hydroxytyrosol Loaded Chitosan Nanoparticles. J Pharm Sci 2015;104:4276–86. doi:10.1002/jps.24666.

[52] Qi J, Zhuang J, Lu Y, Dong X, Zhao W, Wu W. In vivo fate of lipid-based nanoparticles. Drug Discov Today 2017;22:166–72. doi:10.1016/J.DRUDIS.2016.09.024.

[53] Taguet A. Rheological characterization of compatibilized polymer blends. Compat. Polym. Blends Micro Nano Scale Phase Morphol. Interphase Charact. Prop., Elsevier; 2019, p. 453–87. doi:10.1016/B978-0-12-816006-0.00016-5.

[54] Abraham J, Sharika T, Mishra RK, Thomas S. Rheological characteristics of nanomaterials and nanocomposites. Micro Nano Fibrillar Compos. (MFCs NFCs) from Polym. Blends, Elsevier Inc.; 2017, p. 327–50. doi:10.1016/B978-0-08-101991-7.00014-5.

[55] Batchelor AW, Chandrasekaran M. Biotribology of Medical Implants. Frict. Lubr. Wear Technol., ASM International; 2018, p. 372–8. doi:10.31399/asm.hb.v18.a0006404.

[56] Sahoo P, Das SK, Paulo Davim J. Tribology of materials for biomedical applications. Mech. Behav. Biomater., Elsevier; 2019, p. 1–45. doi:10.1016/B978-0-08-102174-3.00001-2.

[57] Dong HS, Qi SJ. Realising the potential of graphene-based materials for biosurfaces – A future perspective. Biosurface and Biotribology 2015;1:229–48.

doi:10.1016/j.bsbt.2015.10.004.

[58] Stachowiak GW, Batchelor AW. Engineering Tribology: Fourth Edition. Elsevier Inc.; 2013. doi:10.1016/C2011-0-07515-4.

[59] Jahanmir S. Future directions in tribology research. J Tribol 1987;109:207–11. doi:10.1115/1.3261335.

[60] Zhou ZR, Jin ZM. Biotribology: Recent progresses and future perspectives. Biosurface and Biotribology 2015;1:3–24. doi:10.1016/j.bsbt.2015.03.001.

[61] Liu X, Xu N, Li W, Zhang M, Chen L, Lou W, et al. Exploring the effect of nanoparticle size on the tribological properties of SiO2 / polyalkylene glycol nanofluid under different lubrication conditions. Tribol Int 2017;109:467–72. doi:10.1016/j.triboint.2017.01.007.

[62] Timm K, Myant C, Spikes HA, Grunze M. Particulate lubricants in cosmetic applications. Tribol Int 2011;44:1695–703. doi:10.1016/j.triboint.2011.06.017.

[63] Jiao D, Zheng S, Wang Y, Guan R, Cao B. The tribology properties of alumina / silica composite nanoparticles as lubricant additives. Appl Surf Sci 2011;257:5720–5. doi:10.1016/j.apsusc.2011.01.084.

[64] Darminesh SP, Sidik NAC, Najafi G, Mamat R, Ken TL, Asako Y. Recent development on biodegradable nanolubricant: A review. Int Commun Heat Mass Transf 2017;86:159–65. doi:10.1016/j.icheatmasstransfer.2017.05.022.

[65] Sarkar A, Andablo-Reyes E, Bryant M, Dowson D, Neville A. Lubrication of soft oral surfaces. Curr Opin Colloid Interface Sci 2019;39:61–75. doi:10.1016/j.cocis.2019.01.008.

[66] Martínez-Acevedo L, Zambrano-Zaragoza M de la L, Vidal-Romero G, Mendoza-Elvira S, Quintanar-Guerrero D. Evaluation of the lubricating effect of magnesium stearate and glyceryl behenate solid lipid nanoparticles in a direct compression process. Int J Pharm 2018;545:170–5. doi:10.1016/j.ijpharm.2018.05.002.

[67] Singh A, Chauhan P, Mamatha TG. A review on tribological performance of lubricants with nanoparticles additives. Mater Today Proc 2019. doi:10.1016/j.matpr.2019.07.245.

[68] Dai W, Kheireddin B, Gao H, Liang H. Roles of nanoparticles in oil lubrication. Tribol Int 2016;102:88–98. doi:10.1016/j.triboint.2016.05.020.

[69] Souto EB, Muller RH. Cosmetic features and applications of lipid nanoparticles (SLN , NLC). Int J Cosmet Sci 2008;30:157–65. doi:10.1111/j.1468-2494.2008.00433.x.

[70] Nakano K, Kobayashi K, Nakao K, Tsuchiya R, Nagai Y. Tribological method to objectify similarity of vague tactile sensations experienced during application of liquid cosmetic foundations. Tribol Int 2013;63:8–13. doi:10.1016/j.triboint.2012.02.011.

[71] Seetapan N, Bejrapha P, Srinuanchai W, Ruktanonchai UR. Rheological and morphological characterizations on physical stability of gamma-oryzanol-loaded solid lipid nanoparticles (SLNs). Micron 2010;41:51–8. doi:10.1016/j.micron.2009.08.003.

[72] Charles Ross & Son Company. New technologies for continuous mixing and homogenization of nano-filled materials Shear-intensive mixing. 2015.

[73] Hajj Ali H, Michaux F, Bouelet Ntsama IS, Durand P, Jasniewski J, Linder M. Shea butter solid nanoparticles for curcumin encapsulation: Influence of nanoparticles size on drug loading. Eur J Lipid Sci Technol 2016;118:1168–78. doi:10.1002/ejlt.201500348.

[74] Svahn F, Kassman-Rudolphi Å, Wallén E. The influence of surface roughness on friction and wear of machine element coatings. Wear 2003;254:1092–8. doi:10.1016/S0043-1648(03)00341-7.

[75] The dependence of friction on surface roughness. Proc R Soc London Ser A Math Phys Sci 1959;252:35–44. doi:10.1098/rspa.1959.0134.

[76] Rheometry - Soft-Matter n.d. http://soft-

matter.seas.harvard.edu/index.php/Rheometry (accessed November 21, 2020).

[77] Chand N, Fahim M. Green tribology and tribological characterization of biocomposites. Tribol. Nat. Fiber Polym. Compos., Elsevier; 2021, p. 207–12. doi:10.1016/b978-0-12-818983-2.00009-8.

[78] Upadhyay R, Chen J. Rheology and tribology assessment of foods: A food oral processing perspective. Biopolym. Formul. Biomed. Food Appl., Elsevier; 2020, p. 697–715. doi:10.1016/B978-0-12-816897-4.00028-X.

[79] Sharma M, Sharma H, Shannigrahi S. Tribology of advanced composites/biocomposites materials. Biomed. Compos., Elsevier; 2017, p. 413–29. doi:10.1016/b978-0-08-100752-5.00018-4.

[80] Prakash S. From Rheology to Tribology: Applications of Tribology in Studying Food Oral Processing and Texture Perception. Adv. Food Rheol. Its Appl., Elsevier Inc.; 2017, p. 65–86. doi:10.1016/B978-0-08-100431-9.00004-8.

[81] Mann A, Tighe BJ. Ocular biotribology and the contact lens: Surface interactions and ocular response. Biomater. Regen. Med. Ophthalmol. Second Ed., Elsevier Inc.; 2016, p. 45–74. doi:10.1016/B978-0-08-100147-9.00003-1.

[82] Mahdi MH, Conway BR, Mills T, Smith AM. Gellan gum fluid gels for topical administration of diclofenac. Int J Pharm 2016;515:535–42. doi:10.1016/j.ijpharm.2016.10.048.

[83] Sahin M, Çetinarslan CS, Akata HE. Effect of surface roughness on friction coefficients during upsetting processes for different materials. Mater Des 2007;28:633–40. doi:10.1016/j.matdes.2005.07.019.

[84] Tribo-Rheometry Accessory – TA Instruments n.d. https://www.tainstruments.com/tribo-rheometry-accessory/ (accessed November 21, 2020).

[85] Cheung CCL, Al-Jamal WT. Sterically stabilized liposomes production using staggered herringbone micromixer: Effect of lipid composition and PEG-lipid content. Int J Pharm 2019;566:687–96. doi:10.1016/j.ijpharm.2019.06.033.

[86] Oliveira DRB, Furtado G de F, Cunha RL. Solid lipid nanoparticles stabilized by sodium caseinate and lactoferrin. Food Hydrocoll 2019;90:321–9. doi:10.1016/j.foodhyd.2018.12.025.

[87] Mohammad Y, Fallah AB, Reynolds JNJ, Boyd BJ, Rizwan SB. Steric stabilisers govern the colloidal and chemical stability but not in vitro cellular toxicity of linoleoylethanolamide cubosomes. Colloids Surfaces B Biointerfaces 2020;192:111063. doi:10.1016/j.colsurfb.2020.111063.

[88] Sun X, Pan C, Ying Z, Yu D, Duan X, Huang F, et al. Stabilization of zein nanoparticles with k-carrageenan and tween 80 for encapsulation of curcumin. Int J Biol Macromol 2020;146:549–59. doi:10.1016/j.ijbiomac.2020.01.053.

[89] Deshpande A, Mohamed M, Daftardar SB, Patel M, Boddu SHS, Nesamony J. Solid Lipid Nanoparticles in Drug Delivery: Opportunities and Challenges. 2017. doi:10.1016/B978-0-323-42978-8.00012-7.

[90] Talele P, Sahu S, Mishra AK. Physicochemical characterization of solid lipid nanoparticles comprised of glycerol monostearate and bile salts. Colloids Surfaces B Biointerfaces 2018;172:517–25. doi:10.1016/j.colsurfb.2018.08.067.

[91] Rigon RB, Gonçalez ML, Severino P, Alves DA, Santana MHA, Souto EB, et al. Solid lipid nanoparticles optimized by 22 factorial design for skin administration: Cytotoxicity in NIH3T3 fibroblasts. Colloids Surfaces B Biointerfaces 2018;171:501–5. doi:10.1016/j.colsurfb.2018.07.065.

[92] Al-Heibshy FNS, Başaran E, Arslan R, Öztürk N, Erol K, Demirel M. Physicochemical characterization and pharmacokinetic evaluation of rosuvastatin calcium incorporated solid lipid nanoparticles. Int J Pharm 2020;578:119106. doi:10.1016/j.ijpharm.2020.119106.

[93] Oliveira RR, Carrião MS, Pacheco MT, Branquinho LC, de Souza ALR, Bakuzis AF, et al. Triggered release of paclitaxel from magnetic solid lipid nanoparticles by magnetic hyperthermia. Mater Sci Eng C 2018;92:547–53. doi:10.1016/j.msec.2018.07.011.

[94] Mazuryk J, Deptuła T, Polchi A, Gapiński J, Giovagnoli S, Magini A, et al. Rapamycin-loaded solid lipid nanoparticles: Morphology and impact of the drug loading on the phase transition between lipid polymorphs. Colloids Surfaces A Physicochem Eng Asp 2016;502:54–65. doi:10.1016/j.colsurfa.2016.05.017.

[95] Shahgaldian P, Quattrocchi L, Gualbert J, Coleman AW, Goreloff P. AFM imaging of calixarene based solid lipid nanoparticles in gel matrices. Eur J Pharm Biopharm 2003;55:107–13. doi:10.1016/S0939-6411(02)00123-6.

[96] Corzo C, Meindl C, Lochmann D, Reyer S, Salar-Behzadi S. Novel Approach for Overcoming the Stability Challenges of Lipid-Based Excipients. Part 3: Application of Polyglycerol Esters of Fatty Acids for the next generation of solid lipid nanoparticles. Eur J Pharm Biopharm 2020. doi:10.1016/j.ejpb.2020.04.027.

[97] Andrade LN, Marques C, Barbosa T, Santos R, Chaud MV, da Silva CF, et al. Praziquantel-loaded solid lipid nanoparticles: Production, physicochemical characterization, release profile, cytotoxicity and in vitro activity against Schistosoma mansoni. J Drug Deliv Sci Technol 2020;58:101784. doi:10.1016/j.jddst.2020.101784.

[98] Müller RH, Petersen RD, Hommoss A, Pardeike J. Nanostructured lipid carriers (NLC) in cosmetic dermal products. Adv Drug Deliv Rev 2007;59:522–30. doi:10.1016/j.addr.2007.04.012.

[99] Fang JY, Fang CL, Liu CH, Su YH. Lipid nanoparticles as vehicles for topical psoralen delivery: Solid lipid nanoparticles (SLN) versus nanostructured lipid carriers (NLC). Eur J Pharm Biopharm 2008;70:633–40. doi:10.1016/j.ejpb.2008.05.008.

[100] Bunjes H, Koch MHJ, Westesen K. Effect of particle size on colloidal solid triglycerides. Langmuir 2000;16:5234–41. doi:10.1021/la990856l.

[101] Hajj Ali H, Michaux F, Khanji AN, Jasniewski J, Linder M. Chitosan - Shea butter solid nanoparticles assemblies for the preparation of a novel

nanoparticles in microparticles system containing curcumin. Colloids Surfaces A Physicochem Eng Asp 2018;553:359–67. doi:10.1016/j.colsurfa.2018.05.075.

[102] Wadetwar RN, Agrawal AR, Kanojiya PS. In situ gel containing Bimatoprost solid lipid nanoparticles for ocular delivery: In-vitro and ex-vivo evaluation. J Drug Deliv Sci Technol 2020;56. doi:10.1016/j.jddst.2020.101575.

[103] Mendonsa NS, Pradhan A, Sharma P, Prado RMB, Murthy SN, Kundu S, et al. A quality by design approach to develop topical creams via hot-melt extrusion technology. Eur J Pharm Sci 2019;136:104948. doi:10.1016/j.ejps.2019.06.002.

[104] Sharma V, Timmons RB, Erdemir A, Aswath PB. Interaction of plasma functionalized TiO2 nanoparticles and ZDDP on friction and wear under boundary lubrication. Appl Surf Sci 2019;489:372–83. doi:10.1016/j.apsusc.2019.05.359.

[105] Sanukrishna SS, Vishnu S, Krishnakumar TS, Jose Prakash M. Effect of oxide nanoparticles on the thermal, rheological and tribological behaviours of refrigerant compressor oil: An experimental investigation. Int J Refrig 2018;90:32–45. doi:10.1016/j.ijrefrig.2018.04.006.

[106] Kerni L, Raina A, Haq MIU. Friction and wear performance of olive oil containing nanoparticles in boundary and mixed lubrication regimes. Wear 2019;426–427:819–27. doi:10.1016/j.wear.2019.01.022.

[107] Thapliyal P, Kumar A, Thakre GD, Jain AK. Investigation of Rheological Parameters of Lubricants and Contact Fatigue Behavior of Steel in the Presence of Cu Nano-Particles. Macromol Symp 2017;376:1700011. doi:10.1002/masy.201700011.

[108] Wang Y, Wu X, Yang W, Zhai Y, Xie B, Yang M. Aggregate of nanoparticles: Rheological and mechanical properties. Nanoscale Res Lett 2011;6:114. doi:10.1186/1556-276X-6-114.

[109] Sajeeb A, Krishnan Rajendrakumar P. Investigation on the rheological behavior of coconut oil based hybrid CeO 2 /CuO nanolubricants. J Eng Tribol

2018:1–8. doi:10.1177/1350650118772149.

[110] Kaganyuk M, Mohraz A. Role of particles in the rheology of solid-stabilized high internal phase emulsions. J Colloid Interface Sci 2019;540:197–206. doi:10.1016/j.jcis.2018.12.098.

[111] Cui Y, Ding M, Sui T, Zheng W, Qiao G, Yan S, et al. Role of nanoparticle materials as water-based lubricant additives for ceramics. Tribol Int 2020;142:105978. doi:10.1016/j.triboint.2019.105978.

[112] Godoi FC, Bhandari BR, Prakash S. Tribo-rheology and sensory analysis of a dairy semi-solid. Food Hydrocoll 2017;70:240–50. doi:10.1016/j.foodhyd.2017.04.011.

[113] Peña-Parás L, Maldonado-Cortés D, Taha-Tijerina J. Eco-friendly nanoparticle additives for lubricants and their tribological characterization. Handb. Ecomater., vol. 5, Springer International Publishing; 2019, p. 3247–67. doi:10.1007/978-3-319-68255-6_72.

[114] Srivyas P, Charoo M, Dev Srivyas P. Tribology in Industry A Review on Tribological Characterization of Lubricants with Nano Additives for Automotive Applications 2018;594:594–623. doi:10.24874/ti.2018.40.04.08.

[115] Pond D, Limbert G, Masen MA, Pond D, Graham HK, Sherratt MJ, et al. Biotribology of the Ageing Skin — Why We Should Care Biotribology Biotribology of the ageing skin — Why we should care. Biotribology 2019;17:75–90. doi:10.1016/j.biotri.2019.03.001.

[116] Huang X, Chau Y. Investigating impacts of surface charge on intraocular distribution of intravitreal lipid nanoparticles. Exp Eye Res 2019;186. doi:10.1016/j.exer.2019.107711.

[117] Du Y, Ling L, Ismail M, He W, Xia Q, Zhou W, et al. Redox sensitive lipid-camptothecin conjugate encapsulated solid lipid nanoparticles for oral delivery. Int J Pharm 2018;549:352–62. doi:10.1016/j.ijpharm.2018.08.010.

[118] Peng JQ, Fumoto S, Suga T, Miyamoto H, Kuroda N, Kawakami S, et al.

Targeted co-delivery of protein and drug to a tumor in vivo by sophisticated RGD-modified lipid-calcium carbonate nanoparticles. J Control Release 2019;302:42–53. doi:10.1016/j.jconrel.2019.03.021.

[119] Chee PN, Pun SH. A perfusable 3D cell-matrix tissue culture chamber for in situ evaluation of nanoparticle vehicle penetration and transport. Biotechnol Bioeng 2008;99:1490–501. doi:10.1002/bit.21698.

[120] Trombino S, Russo R, Mellace S, Varano GP, Laganà AS, Marcucci F, et al. Solid lipid nanoparticles made of trehalose monooleate for cyclosporin-A topic release. J Drug Deliv Sci Technol 2019;49:563–9. doi:10.1016/j.jddst.2018.12.026.

[121] Abumanhal-Masarweh H, da Silva D, Poley M, Zinger A, Goldman E, Krinsky N, et al. Tailoring the lipid composition of nanoparticles modulates their cellular uptake and affects the viability of triple negative breast cancer cells. J Control Release 2019;307:331–41. doi:10.1016/j.jconrel.2019.06.025.

[122] Suñé-Pou M, Limeres MJ, Nofrerias I, Nardi-Ricart A, Prieto-Sánchez S, El-Yousfi Y, et al. Improved synthesis and characterization of cholesteryl oleate-loaded cationic solid lipid nanoparticles with high transfection efficiency for gene therapy applications. Colloids Surfaces B Biointerfaces 2019;180:159–67. doi:10.1016/j.colsurfb.2019.04.037.

[123] Lee SE, Lee CD, Ahn J Bin, Kim DH, Lee JK, Lee JY, et al. Hyaluronic acid-coated solid lipid nanoparticles to overcome drug-resistance in tumor cells. J Drug Deliv Sci Technol 2019;50:365–71. doi:10.1016/j.jddst.2019.01.042.